DEVELOPMENT AND EVALUATION OF PRECISE POINT POSITIONING FOR TIME AND FREQUENCY TRANSFER

by

Carlos Alexandre Garcia

B.Sc.E. in Geomatics Engineering, Unesp-Brazil, 2006

A THESIS SUBMITTED IN PARTIAL FULFILLMENT OF THE REQUIREMENTS FOR THE DEGREE OF

Master of Science in Engineering

In the Graduate Academic Unit of Geodesy and Geomatics Engineering

Supervisor(s):	Marcelo C. Santos, Dept. of Geodesy and Geomatics Engineering
Examining Board:	Peter Dare, Dept. of Geodesy and Geomatics Engineering
External Examiner:	Christopher Diduch, Dept. of Electrical and Computer Engineering

This thesis is accepted by the

Dean of Graduate Studies

THE UNIVERSITY OF NEW BRUNSWICK

February, 2015

Abstract

Time and frequency became a very important subject in a world that is rapidly changing the flow of gathering, organizing and monitoring information, such as power lines, communication and positioning systems. The higher the uncertainty level of time and frequency stability over a certain period of time, the faster we can gather, organize and monitor the flow of the information/data. Since the 1980's different methods using different combinations of GNSS signals have been developed to achieve the best time and frequency accuracy. This work will present an assessment of the Precise Point Positioning (PPP) software called GPS Analysis and Positioning Software (GAPS) as a tool for time and frequency transfer. GAPS has received many updates to adjust the software to the start-of-the-art of PPP time transfer, providing a relative frequency stability of better than 10^{-14}. The tests in this work showed that GAPS is capable of achieving a link frequency stability of 10^{-15} in both short and long term. The updates involve not only mathematical models, but also the functionality of the software, adding an interface and options capable of computing time links and frequency stability

analyses, all in one software. This new adapted version of GAPS for time transfer is named GAPSTFT.

Dedication

To my family (Eni, Francisco, Alessandra, Wesley and Cesar)

Para a minha familia (Eni, Francisco, Alessandra, Wesley e Cesar)

Acknowledgements

This work was not completed without the help of many other people.

My supervisor Marcelo Santos: You have provided me with more opportunities than I could have imagined. Thank you for believing in me, supporting me, and helping me along the way. I will never forget it. Also, I would like to give a special thanks to:

- Rodrigo Leandro for helping me to understand GAPS source code.
- Felipe Geremia Nievinski for helping me with MATLAB for many years.
- Doctor Joao Carlos Chaves for introducing me to Doctor Santos.
- All the staff from the Geodesy and Geomatics Engineering Department.
- Marcos Mendenco for all the support in many ways.
- Giancarlo Cerretto for answering all my questions about Time and Frequency Transfer
- Paul Girouard for being an incredible friend all these years.

- Gayle MacDonald for all the support and love.
- Dr. M Barghava for changing my life for the better.

Table of Contents

List of Tables

List of Figures

List of Symbols, Nomenclature and Abbreviations

ϕ_{if}	Ionosphere-free combination of carrier-phase measurement
P_{if}	Ionosphere-free combination of the code measurement
ρ	Geometric distance between satellite and receiver antenna
c	Vacuum speed of light
T	Neutral atmosphere delay (troposphere)
dt	Satellite clock offset
dT	Receiver clock offset
λ_{if}	Ionosphere-free effective carrier-phase wavelength
ε_P	Measurement noise components
ε_ϕ	Measurement noise components
N_{if}	Ionosphere-free carrier-phase ambiguity parameter
TEC	Total integrated electron content
f	Frequency of the signal in hertz

I_i	Ionospheric delay
zpd	Zenith path delay
M	Mapping function
X_s, Y_s, Z_s	Satellite coordinates
x, y, z	Station coordinates
A	Design matrix
W	Misclosure vector
δ	Vector of corrections
X	Unknown parameters
P_l	Observation weight
P_{X^0}	A-priori weighted constraint
$C_{\hat{X}}$	Covariance matrix
T	Period
f	frequency
Δ_{AB}	Clock difference between two stations (A and B) using common-view
t_S	Time Signal from a source S (common-view)
d_{SA} and d_{SB}	Path delay for station A and B
Δ_{TD}	Total Delay
INT_{P1}	Receiver and antenna delays for P1 observable
INT_{P2}	Receiver and antenna delays for P2 observable
CAB_D	Antenna cable delay
REF_D	Delay between the external clock and the internal receiver clock

y_i	Frequency value
x_i	First clock phase value
x_{i-1}	Second clock phase value
MAD	Median absolute deviation
$\sigma_y^2(\tau)$	Overlapping Allan Variance
m	Averaging factor
τ_0	Basic measurement interval
M	Fractional frequency values

Chapter 1

Introduction

Time and frequency became a very important subject in a world that is rapidly changing the flow of gathering, organizing and monitoring information.

Power lines use frequency standards to maintain the line frequencies. Computer networks needs to organize their nodes to guarantee the flow of the information. Cellphone towers make use of precise timing to keep the system synchronized. Bank and military communication systems need also precise timing for synchronization of data encryption and decryption. Accurate timing is also the basis for any navigation/positioning systems, such as the Global Positioning System (GPS), Galileo and GLONASS [Jespersen and Fitz-Randolph, 1999].

All of the examples previously mentioned require somehow a combination of precise time and frequency. The higher the uncertainty level of time and frequency stability over a certain period of time, the faster we can gather, organize and monitor the flow of data and the information.

The history of time and frequency transfer has centered on achieving the best accurate time, dissemination and availability between two remote locations. As mentioned before, the accurate timing is part of any global navigation satellite system (GNSS). Each GNSS satellite carries on-board precise atomic clocks, which makes the system capable of disseminating time and frequency around the world 24 hours a day. For those reasons, GNSS has become the primary system for distributing time and frequency. Any facility around the world that can place a GNSS antenna outdoors connected to a GNSS receiver driven by an external atomic clock can synchronize clocks and calibrate and control oscillators [Lombardi et al., 2001].

Since the 1980's different methods using different combinations of GNSS signals have been developed to achieve the best time and frequency accuracy.

A positioning method based on geodetic GNSS receivers and called precise point positioning (PPP) is considered to be the current state-of-the-art method for time and frequency transfer. This method allows us to determine the station clock phase based on the precise products available from the International GNSS Service (IGS). In this way, we can compare clocks around the world using PPP based on the "all-in-view" time and frequency transfer principles.

A PPP software developed at the University of New Brunswick, which is called GAPS (GPS Analysis and Positioning Software), was developed for geodetic positioning purposes.

This work evaluates GAPS as a tool for time and frequency transfer. Some updates and implementations to GAPS were performed to make the software a product focused on time and frequency.

The main research contribution from this work deals with the development and evaluation of the precise point positioning for time and frequency transfer using GAPS software. Evaluation was mainly made possible due to dedicated enhancements in our in-house PPP.

First, we developed and implemented important techniques to assess the time and frequency transfer potential of GAPS, [Orgiazzi et al., 2005] and [Guyennon et al., 2009]. The implementation of the multi-day continues processing highly contributes to achieve better time and transfer results. It not only minimizes the day-boundary-discontinuity problem, but also allows GAPSTFT to perform long-term (up to one year) time and frequency transfer. The long-term time transfer is essential for the time and frequency community allowing them to maintain precise time scales and analyze the behavior of oscillators for long periods. It worth to say that the multi-day processing mode contributes not only for time and frequency transfer, but it also allow GAPS positioning users, to process GNSS data for periods longer than just 24 hours. This contribution has also been implemented on the original GAPS software.

The second contribution part from this work is based on evaluating GAPSTFTs results after its implementations. Evaluating the time and frequency results for short (one day) and long-term (up to one year) term, comparing results to different time and frequency methods and PPP software, allowed us to validate the results and also, understand what type of problem may affect the time and frequency transfer.

At the beginning of the evaluation of the results, we noticed that we had large data set to be processed and different software to be used while performing the desired analysis. The third contribution from this work was to turn GAPS into GAPSTFT, a PPP desktop package focused on providing time and frequency data. GAPSTFT provides not only the estimated time data from a single station as other PPP packages, but it also offers the final time and frequency transfer results between two stations. In addition, as the last contribution, GAPSTFT was updated with tools to perform the most common time and frequency transfer data analysis, [Riley, 2003]. It was not our intention, at the beginning of this work to provide a desktop software at hand, but it ended up helping us to understand about time and frequency Metrology while implementing the tools.

Chapter 2 overviews the theory behind PPP and some concepts of Metrology involving timing and frequency. In Chapter 3, the general theory and techniques of time and frequency transfer using GNSS are presented. Chapter 4 presents GAPS software and its algorithms, as well as, all the updates and implementations made for time and frequency transfer. An interface focused on timing, and tools to evaluate time and frequency stability have also been added to GAPS. After all the updates and implementation, we named this version of GAPS as GAPSTFT (GAPS for Time and Frequency Transfer). In Chapter 5 we do an assessment of GAPSTFT results in different scenarios. Also, a comparison of GAPSTFT with other GNSS time and frequency techniques and other PPP software are presented. Finally, in Chapter 6, we close this work commenting on the results and making recommendations for future developments.

Chapter 2

Background

This chapter describes the theoretical background of precise point Positioning, time and frequency transfer. It is important to have a strong understanding of these three subjects once the focus of this work is to evaluate a PPP software for Time Transfer purpose. Section 2.1 describes briefly the concept of PPP including its mathematical equations and the adjustment procedures. Section 2.2, we discuss the concepts of time and frequency. Section 2.3 presents the basic concepts involving time transfer. Section 2.4 closes this chapter presenting the main idea of Precise Time Transfer.

2.1 Precise Point Positioning

Precise point positioning (PPP) is a technique in which a single receiver is used to determine its coordinates based on the precise orbit and clock products produced by the International GNSS Service (IGS). PPP takes advantage of the precise and accurate carrier phase observations to allow users to obtain positions with centimeter level accuracy.

PPP has been used not only to determine point coordinates, but also as a powerful tool for GNSS data analysis, providing estimation of parameters, such as receiver and satellite clock errors, neutral atmosphere delay, ionospheric delay, code biases, and code multipath.

Many of the error sources that are present in the GNSS observables can be removed by double differences, especially over short distances (less than 10 km). On the other hand, these errors are not removed in PPP, and must be precisely modeled to achieve a comparable level of accuracy.

To achieve the best accuracy on the mentioned parameters estimation, corrections must be applied to the collected observations; such corrections include tides, and relativistic effects among others.

The next sub-sections will present the basic theory related to PPP using the GPS constellation only.

2.1.1 Observation Model

The PPP observation model is nowadays standard. The word standard is being used in this context because most PPP software packages available use the same basic model, with an ionospheric-free combination of pseudorange and carrier-phase [Leandro, 2009].

The basic PPP observation model is presented as:

$$P_{if} = \rho + c(dT - dt) + T + \varepsilon_P \tag{2.1}$$

and

$$\phi_{if} = \rho + c(dT - dt) + T + \lambda_{if} N_{if} + \varepsilon_\phi \tag{2.2}$$

where i represents the carrier-phase measurements on L1 and L2 frequencies; P_{if} and ϕ_{if} are the ionosphere-free combination of code and carrier-phase measurements respectively; ρ is the geometric range (model distance between satellite and receiver antenna); c is the vacuum speed of light; T is the neutral atmosphere delay (troposphere); dt and dT are the satellite and receiver clock offsets respectively; λ_{if} is the ionosphere-free effective carrier-phase wavelength; ε_P and ε_ϕ are the relevant measurement noise components; and N_{if} is the ionosphere-free carrier-phase ambiguity parameter. In this case, the ambiguity is not estimated as fixed integer value, but as a float value.

The ionospheric delay is not present in both equations 2.1 and 2.2; it was eliminated using the iono-free combination of the two frequencies. The ionospheric delay depends on the frequency of the signal, which means that the ionosphere is a dispersive region for radio signals and being inversely proportional to the frequency squared as follows:

$$I_i = \frac{40.3TEC}{f_i^2}, \tag{2.3}$$

where TEC is the total (integrated) electron content and f is the carrier frequency of the signal in hertz.

The carrier phase and pseudorange ionospheric-free combinations can be written respectively as follows:

$$\phi_{if} = \frac{f_1^2}{f_1^2 - f_2^2}\phi_1 - \frac{f_2^2}{f_1^2 - f_2^2}\phi_2, \tag{2.4}$$

and

$$P_{if} = \frac{f_1^2}{f_1^2 - f_2^2}P_1 - \frac{f_2^2}{f_1^2 - f_2^2}P_2. \tag{2.5}$$

Using the so-called precise orbits and clocks, both can be considered as known quantities (as satellite clocks and orbits are not perfectly known residual errors will be present in the estimated values) from the code and carrier-phase measurement equations. Simplified PPP observation equations can be written as:

$$\rho + cdT + T + \varepsilon_P - P_{if} = 0, \tag{2.6}$$

and

$$\rho + cdT + T + N_i\lambda_i + \varepsilon_\phi - \phi_{if} = 0. \tag{2.7}$$

2.1.2 Adjustment Model and Procedure

This section will present the adjustment of the observations used to determine the positioning parameters. The positioning model is divided into the modeled and non-modeled parts. For the adjustment purpose, only the modeled parameters will be taken into consideration, for instance: the zenith troposphere delay, receiver coordinates, the receiver clock error and the carrier-phase ambiguities.

Equations 2.6 and 2.7 will be re-written expressing the tropospheric path delay T as a function of the zenith path delay (zpd) and mapping function (M).

$$\rho + cdT + Mzpd + \varepsilon_P - P_{if} = 0 \tag{2.8}$$

$$\rho + cdT + Mzpd + N_i\lambda_i + \varepsilon_\phi - \phi_{if} = 0 \tag{2.9}$$

The geometric range ρ can be expressed as:

$$\rho = \sqrt{(X_s - x)^2 + (Y_s - y)^2 + (Z_s - z)^2} \tag{2.10}$$

where (X_s, Y_s, Z_s) are the satellite coordinates and (x, y, z) are the station coordinates.

According to [Vanicek and Krakiwsky, 1986], the linearization of observation equations 2.8 and 2.9 around the a-priori parameter values and observations (X^0, l) is represented in matrix form as:

$$A\delta + W - V = 0 \tag{2.11}$$

where A is the design matrix, W is the misclosure vector, V is the vector of residuals and δ is the vector of corrections to the unknown parameter X, which is given as:

$$\delta = -(P_{X^0} + A^T P_l A)^{-1} A^T P_l W, \tag{2.12}$$

and

$$X = \left[x \; y \; z \; dT \; tzd \; N^j_{j=1,nsat} \right]^T. \tag{2.13}$$

Matrix P_l is the observation weight and P_{X^0} is the a-priori weighted constraint. The estimated parameters are:

$$\hat{X} = X^0 + \delta \tag{2.14}$$

with the covariance matrix

$$C_{\hat{X}} = P^{-1}_{\hat{X}} = (P_{X^0} + A^T P_l \, A)^{-1} \tag{2.15}$$

The adjustment procedure is basically a sequential filter, in which the implementation considers the variations in the states of the parameters between epochs and the stochastic process to update their variances [Kouba et al., 2001].

The focus of this research is the term dT (receiver clock), since this parameter will provide the measurements to be used for time transfer. According to [Kouba et al., 2001], the values for the receiver clock will drift according to the quality of its oscillator, e.g. several centimeters/second in the case of an internal quartz clock with frequency stability of about $(10)^{-10}$. The receiver clock process noise can vary as a function of frequency stability but is usually set to white noise with a value to accommodate the unpredictable occurrence of clock resets.

2.1.3 Corrections

Unlike in relative positioning, common errors do not cancel in PPP. In order to have an adequate observation model and achieve the best accuracy, a few corrections must be applied to carrier-phase and pseudorange measurements when using PPP. Below we can see the standard corrections applied to the PPP measurements:

- Satellite ephemeris and clock errors
- Satellite antenna phase center offset and variation
- Phase wind-up error
- Solid Earth tides

- Ocean loading
- Atmospheric loading
- Relativity

Details about each correction applied to any ordinary PPP software can be found in Kouba et al. [2000].

2.2 Fundamentals of time and frequency

The purpose of this section is to consider some concepts and to establish some terminology that will be used later in the discussion of time and frequency transfer.

2.2.1 Time

What is time? Time is commonly used in everyday life; it is not easy to define what time is and it depends on the circumstances and, the a degree of accuracy required when we ask for the time. However, most of the literature defines time as a part of the measuring system used to sequence events or to provide a temporal order of events.

When we think about time and frequency standards in technical terms, these supply three basic types of information: *time-of-day*, *time-interval*, and *frequency* [Lombardi, 2002].

- *time-of-day* is basically provided in hours, minutes and seconds and also it includes the date. Date and time-of-day can also be used to ensure that events are synchronized, or happen at the same time.

- *time-interval*is the duration or elapsed time between two events. Usually the standard unit of time interval is the second. However, engineering applications often require the measurement of shorter time, such as nanoseconds ($1ns = 10^{-9}s$) and picoseconds ($1ps = 10^{-12}s$).

2.2.2 Frequency

The rate of occurrence of a repetitive event is the most simple definition of frequency. If we call T the period of a repetitive event, then the frequency is expressed as $f = 1/T$. As recommended by the international system of units (SI), the period must be expressed in seconds (s) and the frequency in Hertz (Hz) [Lombardi, 2008].

Among the four basic standards of measurement, three of them (length, mass and temperature) hardly achieves the resolution of 1 part per million (10^{-6}). Meanwhile, in time and frequency Metrology measurements of 1 part per billion (10^{-9}) are easily accomplished.

2.2.3 Clock

Clock is a device that displays or records time information. When we use a clock to label an event, the label may be called *timetag* [Lombardi and Nelson, 2001].

Any clock can be considered a two-part device. The first part is used to determine the length of a desired time interval, e.g., a pendulum. This is usually related to as the clock frequency standard. The second part is a counter that keeps track of the number of seconds, or clock cycles, that have occurred, e.g., the gears and clock face in a pendulum clock.

In theory, if a clock were set perfectly and if its frequency/rate remained perfect, it would keep the correct time indefinitely. In real life it is impossible.

In this work, we will present and define some technical terms related to clock and time:

- *Clock-offsets*: are the estimated clocks provided by GAPS. It can be just one value or a sequence of values given the offset value between two clocks.

- *Clock-phase* or just *phase*: is a time series of clock-offset values, after being though the techniques to remove their drifts and outliers, fill the outliers' gaps and apply the internal delays to it. In other words, it is a time series of clock-offset values ready to be used for a time stability analysis or to be converted into frequency.

The quality of a clock depends on how stable and precise its frequency is, and the sensitivity the clock has to environmental changes. Four useful measures for describing the quality of a clock are: frequency accuracy, frequency stability, time accuracy, and time stability.

- *Frequency accuracy* is how well it can realize the defined length of the second
- *Frequency stability* indicates the change in frequency from one period of time to the next. A clock can have a significant frequency error and still be very stable.
- *Time accuracy* by definition means how well a clock agrees with the UTC time scale.
- *Time stability* is usually correlated with frequency stability, but it is often useful as a measure of changes with respect to some uniform flow of time in time-measurement systems and/or time-distribution or time-dissemination systems.

All time and frequency standards are based on a periodic event that repeats at a constant rate. The device that produces this event is called a resonator, e.g., a pendulum. All resonators need an energy source. Taken together, a resonator and the energy source form an oscillator, which can be used to establish a time scale.

2.2.4 Timekeeping

The history of timekeeping started when the location of the sun in the sky was the only reliable indication of time. When the sun was not visible, the time was not know with much precision. To solve that problem, people developed devices (clocks) to interpolate the time between the sunrise and sunset.

Around 3500 B.C, the Egyptians created the so-called shadow clock, which was based on the movement of the sun and its shadow. Since then, clock designers have searched for more stable resonators.

The necessity of measuring time helped advance far the evolution of technology and, as technology improved, more demanding applications were developed.

Around 1955, the first atomic clock was developed by Essen and Parry, which put timekeeping on the hands of Metrology and revolutionized all communication and information systems. Today, the most demanding applications require atomic timekeeping.

2.2.5 Oscillators and frequency standards

Oscillators are defined as an electronic device that generates an oscillating signal. The oscillation is based on a periodic event that repeats at a constant rate. The periodic event is controlled by a resonator, which needs an energy source, so it can keep the oscillation. In other words, the energy source and resonator form an oscillator.

As everything in timekeeping, the oscillators have gone through tremendous developments during the last century. The mechanical oscillators were the most used ones until the beginning of the 1900's. Examples: pendulums, quantum harmonic oscillator, mass on a spring, and vibrating string.

In the present days, there are two main types of oscillators used as frequency standards: quartz oscillators and atomic oscillators.

2.2.5.1 Quartz Oscillators

The first quartz oscillators came out during 1920's and quickly replaced the pendulum devices as standards for time and frequency purposes. There are a large variety of quartz standards, from inexpensive wristwatches to space tracking systems.

Quartz oscillators are very sensitive to environmental parameters such as temperature, humidity, pressure, and vibrations. Once the environmental parameters change, the fundamental resonance frequency also changes.

Aging is another factor that can affect all quartz oscillator. Aging is perceived as a linear change in the resonance frequency and it can be positive or negative. According to [Lombardi, 2008], a high-quality quartz oscillator age at a rate of 5×10^{-9} per year or less.

The best quartz oscillators can achieve a frequency stability as small as 1×10^{-10} and have a good short-term stability (1 day).

2.2.5.2 Atomic Oscillators

The development of radar and high frequency radio communications in the 1930's, 1940's and 1950's made possible the generation of the kind of electromagnetic waves needed to interact with atoms. From those developments, researches developed an atomic clock focused on microwave resonances. In 1949 the first atomic clock was built based on ammonia. The ammonia performance was not better than the existing standards at the time.

The cesium atomic clock replaced by the ammonia in the 1960's, had being refined enough to be incorporated into the official timekeeping systems of many time laboratories.

There are three main types of atomic oscillators: rubidium standards, cesium standards, and hydrogen masers. All the three types work locking their internal quartz oscillator to a resonance frequency generated by the atom of interest. Using this method, all the factors that degrade the quartz oscillator in a long-term disappears. Summarizing, the long-term stability of an atomic oscillator is much better than a quartz oscillator.

According to [HP, 1997], we can define and classify the most used atomic clocks as:

- *Rubidium Oscillators* are the lowest priced atomic oscillator. On the other hand it offers the best price-performance ratio of the other two atomic oscillators.The rubidium frequency is synthesized from a frequency of 5 MHz and the quartz frequency is steered by the rubidium resonance. It leads to a very stable frequency. The result is a stable frequency with the short-term frequency of a quartz oscillator and a better long-term stability.

- *Cesium Oscillators* are the primary and most used frequency standards. Also the SI second is based on the resonance of a cesium oscillator. There are two problems with the cesium oscillators: the cost and the stability over short term. Due to the Cesium oscillators reliability problem, it needs to be regularly monitored to make sure it is still running under cesium expected behavior.

- *Hydrogen Masers* are the most elaborate and expensive frequency standard available commercially. There are two types of hydrogen masers. The first type, called an active maser, oscillates spontaneously and a quartz oscillator is phase-locked to this oscillation. The second type, called a passive maser, its frequency locks a quartz oscillator to the atomic reference.

2.2.6 Time scales

A system of assigning dates to events is called a time scale. There are a number of different time scales. The first time scale was astronomical, based on the apparent motion of stars in the sky.

The necessity of measuring time precisely pushed the evolution of technology and, as technology improved, the astronomical time scales were replaced by the more precise atomic scales. Since atomic time standards were so clearly superior to the astronomical time scales, they were used to define the SI second. Since 1971, the cesium atom has been used to define the second, as: "The second is the duration of 9 192 631 770 periods of the radiation corresponding to the transition between the two hyperfine levels of the ground state of the cesium 133 atom" [HP, 1997].

The next subsections will discuss the most known and used time scales.

2.2.6.1 TAI

The International Atomic Time (TAI) is a uniform time standard generated by atomic clocks located at many timing laboratories around the world.

Metrology laboratories measure their time and frequency and send the measurement data to the Bureau International des Poids et Measures (BIPM) in Sevres, France. BIPM averages the data collected from approximately 200 atomic clocks in 50 laboratories, as a result of this averaging, two time scales are generated, the International Atomic Time (TAI) and Coordinated Universal Time (UTC). Most of these laboratories uses standards base on Cesium, although the number of contributing Hydrogen masers is increasing.

Table 2.1: The Evolution of Clock Design and Performance [Lombardi, 2002]

Type of Clock	**Resonator**	**Date[Ref.]**	**Timing Unct.**	**Frequency Unct**
Sundial	Motion of sum	3500 B. C.	NA	NA
Verge escapement	Verge and foliet mechanism	14th century	15 m	1×10^{-2}
Pendulum	Pendulum	1656	10 s	7×10^{-4}
Harrison chronometer	Pendulum	1761	400 ms	4×10^{-6}
Short pendulum	2 pendula slave and master	1921	10 ms	1×10^{-7}
Quartz crystal	Quartz crystal	1927	100 s	1×10^{-9}
Rubidium gas cell	Rubidium atomic resonance	1958	1 s	1×10^{-11}
Cesium beam	Cesium atomic resonance	1952	10 ns	1×10^{-13}
Hydrogen	Hydrogen atomic resonance	1960	10 ns	1×10^{-13}

2.2.6.2 UTC

Time users always wanted an official time scale that would tie to Earth's rotation. However, it was difficult as the Earth speeds up and slows down. To account for the instability of the Earths spin rate, a time scale called UTC was created employing leap seconds, which are determined by the International Earth Rotation Service (IERS).

According to [HP, 1997], leap seconds are introduced when necessary to keep UTC within 0.9 seconds of Earth time (UT1), and there have been 25 leap seconds added between January 1, 1972 and June 30, 2012. At the estimated rate of decrease, the earth would lose about 1/2 day after 4,000 years, and about two leap seconds a month would be needed to keep UTC in step with UT1.

2.2.6.3 GPS Time

GPS time (GPST) scale is the time scale used for time tagging, or referencing, the GPS satellite signals. It is computed using the atomic clock on board GPS satellites and at the monitor stations on ground.

GPST is considered a continuous time scale because there is no leap seconds added to it [El-Rabbany, 2002]. It means that it will change by 1 second with respect to UTC whenever a leap second is inserted into UTC.

The relationships between the different time scales, in seconds, are given as follows:

$$TAI = GPST - 19.0 \tag{2.16}$$

$$UTC = TAI - (10) \tag{2.17}$$

where (10) in equation 2.17 represents the number of leap seconds currently being used.

2.3 Time Transfer

In this section an overview of synchronization and precise time transfer concepts will be presented.

2.3.1 Why Precise Time, Time Transfer and Synchronization

Precise time, time transfer and synchronization are essential for navigation, communication, power grid, security and many other applications. The clock synchronization ensures that reliable and precise information is transmitted and received inside a system.

The first registers about time synchronization came from maritime navigation. British navigators needed to synchronize their chronometers to a central clock located at Greenwich observatory.

Over time, the variety and number of applications using precise timing has highly increased following improvements in clocks' precision. The arrival of atomic clocks opened new vistas for the applications using clock synchronized systems.

To start to understand what exactly is synchronization and time transfer, we need to go through all the concepts that are part of it.

A precise time is always derived from a time source, which is known as time or (frequency) standard. Sometimes 10^{-10} can be called precise for a system that requires only that precision, but it would not be precise for other systems that requires a higher one.

The idea of performing a synchronization is based in three things. Fist, a reliable time source is needed. Second, a method to transfer the time from the time source to the other clocks has to be chosen according to the accuracy required. Third, the synchronization is performed.

It is very common for many applications to require different clocks at different places to be set to the same time (synchronization). The main goal of time synchronization is to minimize the offset between the local time (users) to a reference time (time source). In this case, the time accuracy of a clock depends on the accuracy and stability of its frequency source, and how its time is periodically adjusted with respect to the reference time source.

The time offset is defined as the difference between a measured on-time pulse $t1$ and an ideal on-time pulse $t2$ that matches exactly with a reference time. Figure 2.1 presents the difference between the $t1$ and $t2$, where the horizontal axis is represented by seconds and the vertical one by a clock phase.

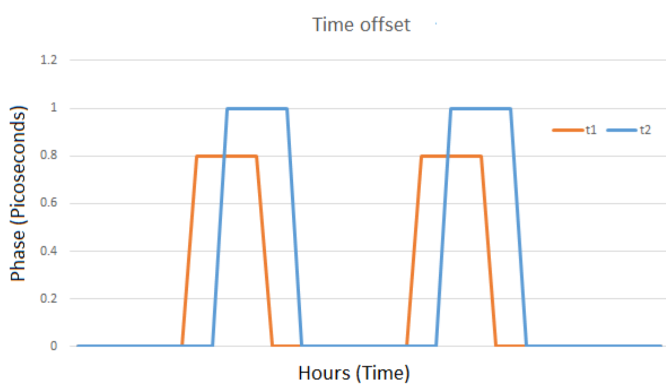

Figure 2.1: Time offset

The frequency offset is defined as the difference between a measured frequency and ideal frequency (standard with zero uncertainty). Figure 2.2 shows the difference between the ideal and measured frequency, characterizing the frequency accuracy/offset.

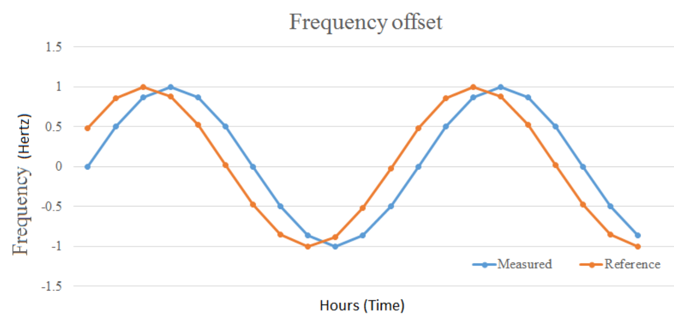

Figure 2.2: Frequency offset

2.3.2 Time Transfer Methods

As already said before, time and frequency is of fundamental importance for science and technology. All the technologies behind time are taken as granted in our daily life. Ship navigation, aircraft, vehicles, wide area networks, high speed INTERNET, digital telecommunication are based on accurate frequency, time and their dissemination.

At distant locations the received frequency and time information allows one to compare, generate or synchronize local time scales, to discipline oscillators or to measure propagation delay times between transmitters an receivers.

The transfer techniques must meet different requirements depending on the method applied to transmit the frequency and/or time. For time transfer, all the contributions to the path delay, as in the cables, equipment and propagation path have to be taken into consideration properly.

Clocks operating in different locations A and B can be compared as said before. The most common ones include transporting one clock or exchanging electromagnetic signals between A and B.

The remaining section in this Chapter will present the most common methods used for dissemination, comparison and synchronization of time and frequency.

2.3.2.1 Portable Clock

The use portable clock is the simplest method to measure time along a path. This method is based on synchronizing a clock to the transmitter. Then, the clock carried to the end of the path, where its time will be compared to the signal sent from the transmitter.

Many timing laboratories used this method in the past. However, this method is very limited due to the frequency stability of the portable clock while it is being transported. Also, many uncertainties are needed to be minimized based on the relativistic corrections.

The portable clock method, has been replaced for the time transfer by electromagnetic signals with radio frequencies or optical frequencies. These methods can differ in expenditure and accuracy: one-way time transfer;

common-view; and two-way time transfer. These methods will be described in the following subsections.

2.3.2.2 One-way Time and Frequency Transfer

Time and frequency transfer can use signals broadcast through many different media, including coaxial cables, optical fiber, radio signals (different spectrum), telephone lines, and INTERNET. The synchronization is required on both time pulse and time code. On the other hand, synchronization will be performed extracting a stable frequency from the carrier itself, or from a time code or other information modulated onto the carrier.

The simplest time transfer method using transmission from a source to a target is called One-Way Time Transfer. On the other hand, it is the most limited in performance. Figure 2.3 shows the in one-way TT.

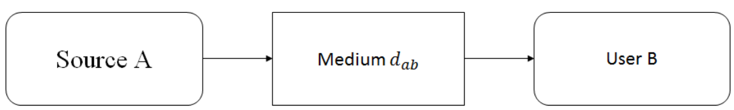

Figure 2.3: One-way time and frequency transfer concept

In this method, a source A (transmitter) sends a time signal to the user called as B. This time in most of the cases is referenced to atomic oscillators. During the transmission there is the delay d_{ab}, commonly called "path delay". In some cases, the correction of this delay is required, unless the accuracy desired is very low or the baseline A and B is very short. For time transfer purpose, the absolute magnitude of the path delay must be known. For frequency transfer, only the variability of the delay (stability) is important.

The NIST Radio Station WWWB, the telephone voice announcements and the Global Positioning System (GPS) are examples of one-way time transfer systems.

The GPS one-way time transfer will be explained in details in Chapters 3.

2.3.2.3 Common-view Time and Frequency Transfer

In the simplest version of common-view, a number of receivers and stations (two or more) receive simultaneously time signals transmitted from a single source. Each receiver measures the time at which a particular signal arrives at its location. The receivers then compare these measurements and subtract them.

According to [Allan et al, 1980], simultaneous observation of the same signal transmitted, for instance, by a satellite and receiver at different locations can be used to synchronize the clocks at the specific locations. Again, consider two stations A and B receiving the clock signal t_S from the source S, over the path $S-A$ and $S-B$ with a clock signal at station A as t_A and at the station B as t_B. The signals also suffers a delay over the paths d_{SA} and d_{SB}.When stations A and B exchange the results (Δ_{AB}) of their measurements $\Delta_{SA} = (t_A - t_S) - d_{SA}$ and $\Delta_{SB} = (t_B - t_S) - d_{SB}$, the resulting equation is:

$$\Delta_{AB} = \Delta_{SA} - \Delta_{SB}, \tag{2.18}$$

$$\Delta_{AB} = [t_A - t_S - d_{SA}] - [t_B - t_S - d_{SB}] = t_A - t_B - [d_{SA} + d_{SB}]. \tag{2.19}$$

The advantage of this method is to avoid the necessity to know the exact time of the clock at the transmitter e.g., located on board of a satellite since t_S is canceled.

Figure 2.4 shows the common-view transfer method.

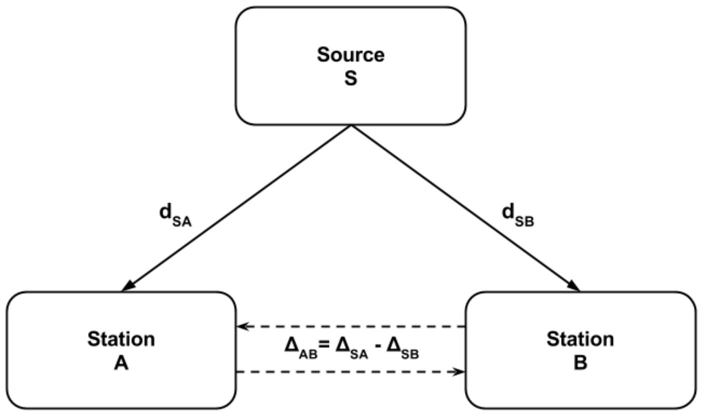

Figure 2.4: Common-view transfer concept

2.3.2.4 Two-way Time and Frequency Transfer

In the two-way time and frequenter transfer method, signals travel both ways between two stations (clock or oscillators) A and B as shown in Figure 2.5. The signal's delay in this method cancels out due to the symmetry of the path between the two stations.

Figure 2.5: Two-way Time Transfer

The delay in this method is estimated as one-half of the measured round trip delay (one-way delay between the A and B). After the estimation, the delay is sent from station B to station A and applied as a correction.

The two-way satellite time and frequency transfer (TWSTFT) technique measures the time interval with respect to the Time Interval Counters (TIC), at each station. Each TIC is started by a pulse from the local clock, then stopped by a pulse from the remote station clock. The same idea happens with the two stations. The measured time interval data are saved at both stations, then exchanges and differenced. To exchange the data a communication system is required.

Figure 2.6 presents the TWSTFT method using a geostationary communication satellite.

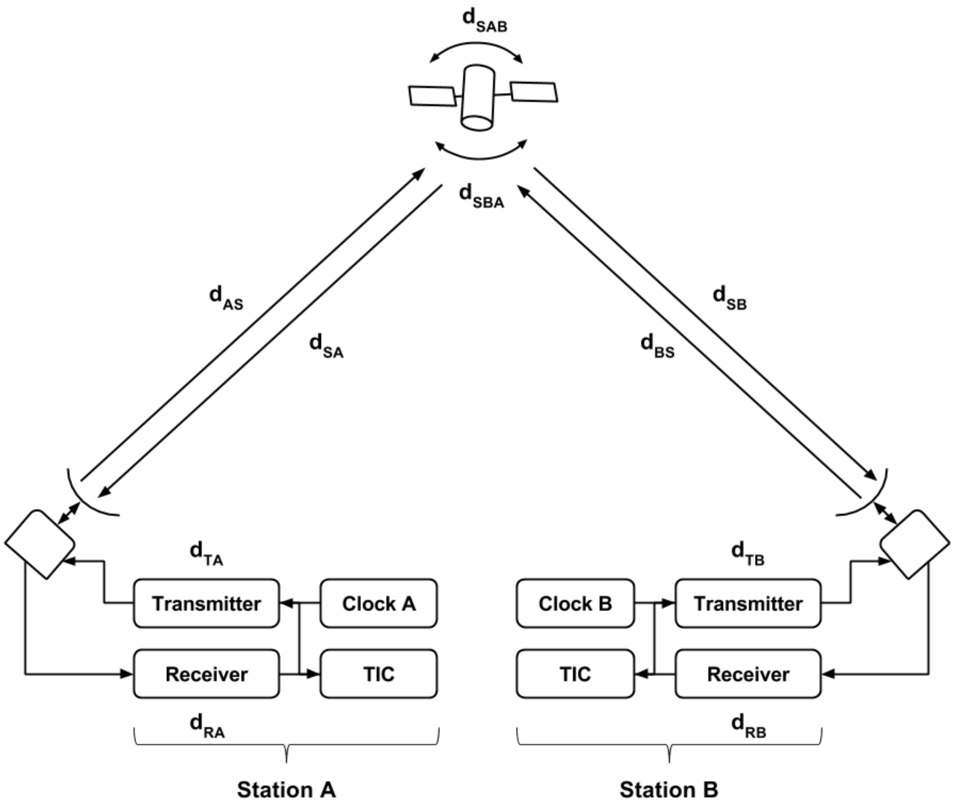

Figure 2.6: Two-way Satellite Time Transfer

The comparison between the two clocks from both Station A and B is presented by the equations 2.20, and 2.21:

$$TIC(A) = A - B + d_{TB} + d_{BS} + d_{SBA} + d_{SA} + d_{RA} + SB \qquad (2.20)$$

$$TIC(B) = B - A + d_{TA} + d_{AS} + d_{SAB} + d_{SB} + d_{RB} + SA \qquad (2.21)$$

The parameters $TIC(A)$ and $TIC(B)$ are the time interval counter, A and B are the respective clock times. The parameters starting with d_{xx} are propagation delays illustrated in Figure 2.6. Based on equations 2.20 and 2.21, we can calculate the difference between the clocks $(A - B)$ as shown in equation 2.22:

$$\begin{gathered} A - B = \frac{[TIC(A) - TIC(B)]}{2} \\ + \frac{(d_{TA} - d_{RA})}{2} - \frac{(d_{TB} - d_{RB})}{2} \\ + \frac{(d_{AS} - d_{SA})}{2} - \frac{(d_{BS} - d_{SB})}{2} \\ + \frac{(d_{SAB} - d_{SBA})}{2} \\ - \frac{2\omega Ar}{2} \end{gathered} \tag{2.22}$$

The last term is the Sagnac effect of the rotating Earth where ω is the angular velocity of the earth, c is the speed of light, and Ar is the area defined by the projections onto the equatorial plane by the line segments connecting the satellite and the earth's center to the two earth stations.

2.4 Summary

Chapter 2 reviewed the theory behind PPP concept. The basic observations equations were presented. As this thesis merges two different science fields, geodesy and Metrology, a basic review of time, frequency and time transfer was presented. The two reviews will be very useful when the two subjects get merged in the following chapters.

Chapter 3

Using Geodetic Receivers for Time and Frequency Transfer

As mentioned in the previous chapters, the number and variety of applications using precise timing has increased, and still increases, very fast. Precise timing is the heart of managing the flow of information around the globe.

The time community is always looking for reliable, robust and inexpensive ways of managing time to be used in synchronized systems.

The Global Positioning System is a classic example of using precise timing from a high-end technology system. GPS features a set of more than 24 orbiting satellites in the sky, each one with synchronized atomic clocks on board. That gives GPS the capacity of providing timing at any point of the Earth, at any time from at least four satellites. Even though GPS was created to be a navigation system providing location, the precise timing is also embedded as part of its technology, making it a perfect system for timing and frequency dissemination due to its availability and quality. No previous system has provided this potential combination of accuracy and availability.

3.1 GNSS Receiver Equipment for Timing

There are several types of GNSS receivers used in time and frequency Metrology. They have different cost, size and design, but most of them share many common features.

Some GNSS timing receivers can provide time-of-day information in a digital format, typically using a RS-232 interface or similar. The time and frequency are provided by averaging all the satellites in view. Usually the receiver provides a 1 pulse per second (pps) electrical output, which can easily be synchronized to within 100 ns of UTC by entering a delay constant that compensates for the antenna, antenna cable and receiver delays.

Another type of GNSS timing receiver is called GNSS disciplined oscillators (GPSDO). They can provide not only the on-time pulse and time-of-day information, but also, can provide the standard frequencies. Typically, they have outputs at 5 MHz and/or 10 MHz, but sometimes they can provide frequencies used in telecommunications, such as 1.44 or 2.048 MHz. These type of receivers work with a high-quality local oscillator, such as an oven controlled quartz crystal (OCXO) or rubidium. There are many applications for the GPSDOs receivers. For instance, they can be used as references for frequency calibrations, to distribute frequency inside a facility, as an external time base oscillator for testing counters and signal generators or they also can be used in telecommunications applications [Lombardi and Nelson, 2001].

Another type of GNSS receiver is the one designed for geodetic and surveying applications. Usually, these receivers are more expensive than the previously mentioned timing GNSS receivers.

This chapter will provide a deeper understanding of how the GPS or any GNSS system can be used for precise timing using geodetic methods. In the next sections, the main GNSS methods used for time transfer will also be discussed, but the focus will be placed on using the geodetic GNSS receivers for precise timing.

3.1.1 GNSS geodetic receivers for timing

As mentioned before, using GNSS geodetic receivers we can estimate its position performing the least-squares adjustment of the observations. But the receiver's position is not the only parameters we can estimate. Parameter related to receiver clock, atmospheric delays, and carrier phase ambiguities can also be estimated or modeled as well.

At the beginning of the 1980's, the time community started to use GNSS receivers to estimate the receiver clock and then perform clock comparisons. At that time, the first GPS receiver used for timing purpose was the one called single-channel and single-frequency, which was able to track only the C/A code of a single satellite at each time.

Later on, at the end of 1990's, geodetic GPS receivers, called multi-channel, started to be used by the time community. These receivers were capable of tracking the P code and the C/A code on both carriers. A geodetic time transfer system (GETT) uses geodetic receivers, models and software developed for high-precision positioning to estimate clock behavior [Plumb et al, 2002].

The ideal GETT setup for timing would be disconnecting the internal quartz oscillator and use an external atomic oscillator/clock is used to steer the receiver frequency. Also, it re-synchronize its internal 1 pps on the 1 pps signal provided by the external clock. In this way, we have the internal receiver timing mirroring the external clock, which can be chosen as UTC(k), where k is the local laboratory clock time. Figures 3.1 and 3.2 show examples of an estimated receiver clock with and without an external atomic oscillator respectively.

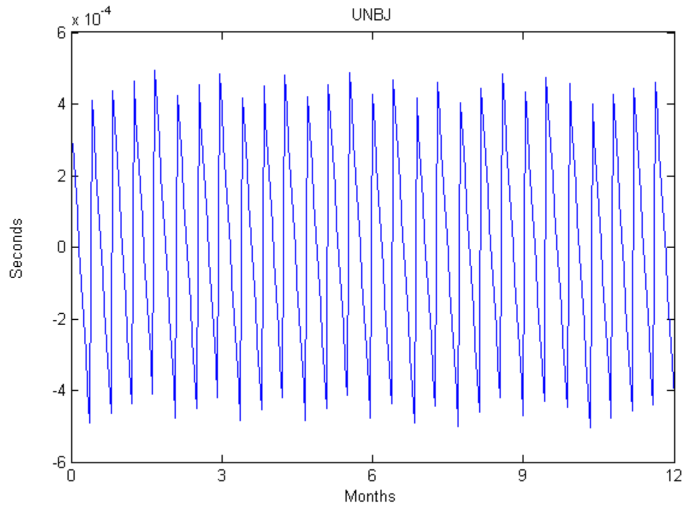

Figure 3.1: Example of GPS clock offset estimation driven by an internal quartz clock

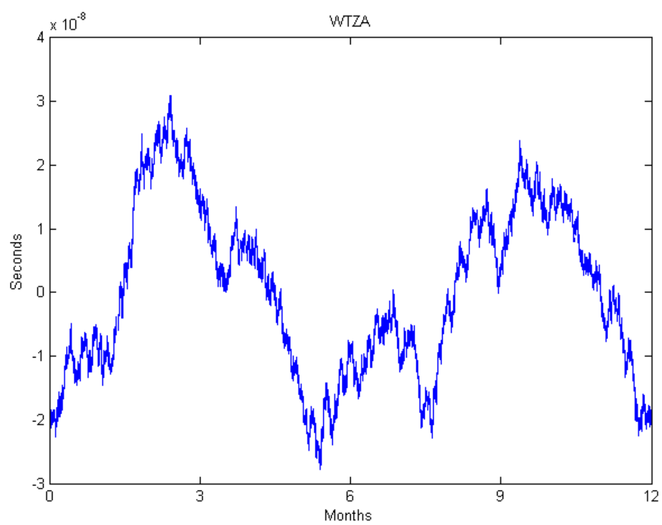

Figure 3.2: Example of GPS clock offset estimation driven by an external atomic clock

There is another type of geodetic receiver which does not accept the 1 pps input. In that case, a Time Interval Counter (TIC) is necessary to compute the clock offsets between the receiver clock (1 pps output) and the external clock corresponding to UTC(k) [Defraigne et al, 2002]. Figure 3.3 shows a traditional example of a time and frequency transfer based on geodetic receivers boards.

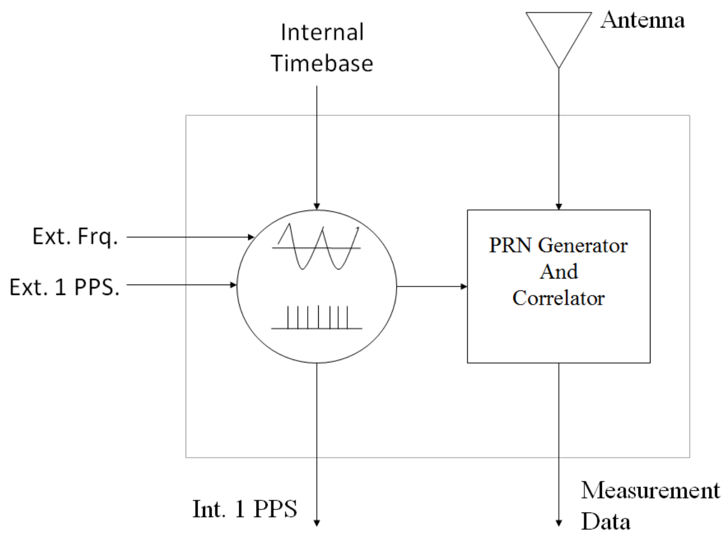

Figure 3.3: Time and frequency transfer setup based on geodetic receivers [Feldmann, 2011]

In parallel with the effort to have the best GNSS receiver for timing, there have been other efforts to develop the current GNSS measurement and modeling techniques.

3.2 GNSS Measurements and Modeling Techniques for clock comparison

As we have different options of geodetic receiver for timing, we also have different measurements and modeling techniques. According to Lombardi and Nelson [2001], there are three different types of GNSS measurement for timing: one-way, common-view and all-in-view. However, the common-view and the all-in-view methods are the two methods currently used by the time community.

The next subsection will present a better understanding of measurements and modeling techniques used with geodetic receivers for timing purposes.

3.2.1 GNSS common-view (CV)

The GNSS common-view (CV) is a well-established method to compare two clocks and/or oscillators located in different places (time and frequency transfer). Back in the 1980's, the GNSS common-view method was performed using only single-channel GPS receivers. Since the end of 1990's, the multichannel geodetic GNSS receivers started to replace the single-channel ones, when performing the common-view method.

When comparing two clocks located in different locations using common-view, the main idea is to make sure that at least one satellite is in common-view between the two locations. Figure 3.4 shows the concept of the GNSS time and frequency transfer using common-view measurement method.

Below we present the CV measurement and modeling in two parts.

The measurement concept lies on having the two receivers collecting data from all satellites in common view. The geodetic receivers must have an external clock time and frequency signals, as 1 pps and 10 MHz.

The satellites are in common view of both receivers, and their signals are simultaneously received by both. Each receiver compares their received signals to its local clock and records the data.

For a simple example, let us initially present a GNSS common-view with only one satellite S_1 in common-view for the stations A and B. The GNSS receiver located at the station A receives GNSS signals over the path d_{S1-A} and compares the reference clock to its local clock $(S_1 - ClockA)$. Receiver B also compares the reference clock transmitted over the path d_{S1-B} to its local clock $(S_1 - ClockB)$. The final measurement in this case is presented as $(ClockA - ClockB) - (d_{S1-A} - d_{S1-B})$.

Now, let us provide an example more complex of a GNSS common-view using 4 satellites (S_1, S_2, S_3 and S_4) and collecting observations at a rate of 5 seconds for a period of 20 seconds. This example provides us a total of 16 measurements. In other words, we will have 4 measurements (1 measurement for each satellite in-common-view) for each epoch (5, 10, 15 and 20 seconds). Once all the observations are collected and saved, for instance, using the RINEX format.

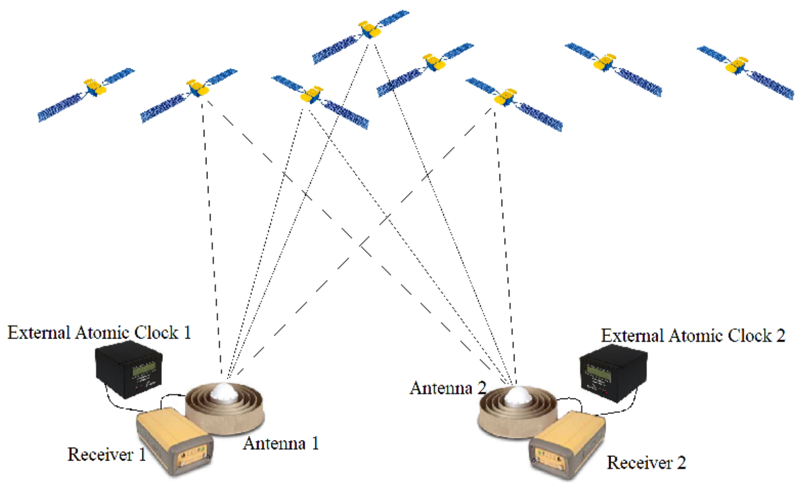

Figure 3.4: Common-view method

The GNSS CV compares measurements collected for the same satellite at the same time. Using this method most of the uncertainties involving the GPS measurements are canceled out. Also, for time and frequency transfer, the receiver, antenna and antenna cable delays and the delay between the external clock and the receiver clock must be apply as a constant. All these delays are constant and they are computed during a calibration process [Plumb et al, 2002]. The corrective term, which takes into account the contribution from all these delays, is called "total delays", and is computed as:

$$\Delta TD_k = [154^2 \times INT_{P1} - 120^2 \times INT_{P2}] \div 9316 + [CAB_D - REF_D] \quad (3.1)$$

where ΔTD_k is the total delays for a specific time laboratory k, INT_{P1} and INT_{P2} are the receiver and antenna delays for P1 and P2 observable, CAB_D is the antenna cable delay, REF_D is the delay between the external clock and the internal receiver clock, and the coefficients 154^2, 120^2, and 9316 are due to the ratio of the two GPS frequencies. All the delays are typically expressed in nanoseconds.

3.2.1.1 Common-view state of art: P3 method

For many years, the standard method to compare clocks and perform time and frequency transfer was the common-view method using only the GPS C/A code observations.

After the end of the 1990's, a new approach to compare clocks based on geodetic receivers driven by an external frequency was developed [Defraigne et al., 2002]. It takes advantage of the P code available on L1 and L2 frequencies. The main idea is to use the RINEX files from the geodetic receivers to process the ionosphere-free combination of the codes P1 and P2 and to use the IGS rapid or precise orbits from IGS and at the same time, following the Common-View approach.

The P3 method rapidly replaced the C/A code method used before. This method presents three advantages over the C/A common-view method. The P3 is more accurate than the broadcast modeled ionospheric delay. The P-code measurements in geodetic receivers have a higher resolution than the C/A measurements. As the geodetic measurements happen many times in 1 second, the P3 method contain less short-term measurement noise.

To estimate the P3 receiver delay, the data recorded in the RINEX file, from both receivers, on both L1 and L2 frequencies, must be taken into account. The main idea of the P3 method is based on the fact that the delay through the ionosphere is proportional to TEC/f^2, where the TEC is the total electron content over the signal path and f is the GPS frequencies.

That being said, the impact of the ionosphere delay can be canceled by the liner combination presented previously as Equation 2.5.

By design, the CV removes and/or reduces common errors between the two observed stations. On the other hand, this technique is limited to long distances between the two stations. Long baselines between the two stations could not provide enough common-view satellites between the two stations.

The next subsection will present the All-in-view technique, which as contrary to the CV, long baselines between the two stations do not affect the quality of the clock prediction.

3.2.2 GPS All-in-View (AV)

The principle of AV is very simple: two stations (time laboratories) collect all the GNSS observations in view, but instead of using the GPS time scale as reference, they use the IGS products as reference, Figure 3.5 illustrate the AV method [Jiang et al., 2004]

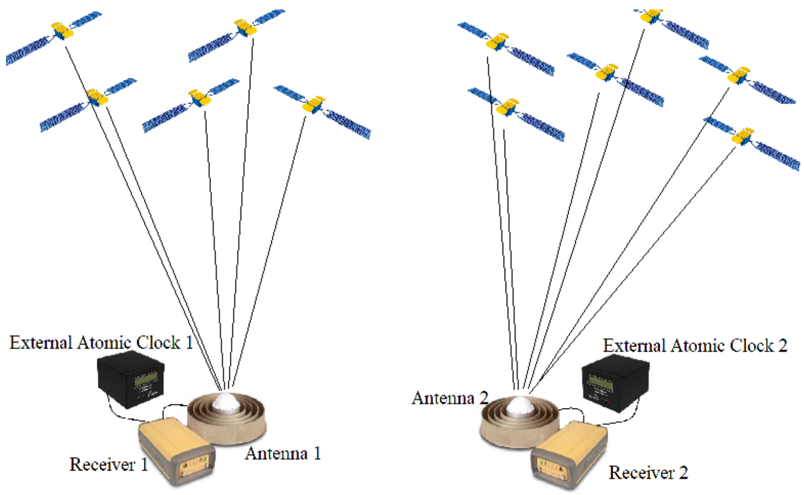

Figure 3.5: All-in-view method

The PPP technique represents well the AV, it uses all the observations in view providing better results. In comparison to CV, the PPP provides some advantages:

- Two clocks can be compared without limits for the baseline length.
- The number of satellites in view with high elevation angle with high signal noise ratio is increased.
- Any clock at any laboratory can be linked and the link is affected only by the equipment.

The AV technique performed as PPP has shown clock solutions consistent with IGS clock products at the sub-nanosecond level and at 2 nanosecond level with the TWSTFT results [Orgiazzi et al., 2005]. The PPP also shows an improvement in stability over two traditional GPS time synchronization methods (single and dual-frequency common view GPS), providing a frequency stability of 10^{-14} (Allan deviation) over a short-term period of one day.

Since the beginning of the 21st century, the timing community started to publish the first results using the PPP as a time transfer tool [Orgiazzi et al., 2005 and Guyennon et al., 2009]. These papers present different strategies to analyze the time and frequency stability using PPP. Petit et al., [2009] introduced the PPP as a new technique to compute the time link for the TAI. After that, different researches, using different PPP software suits, have been used to validate and improve the method.

3.3 Summary

This chapter presented a brief discussion about the different types of GNSS receivers to be used for timing and frequency purposed. After presenting the different receiver types, the chapter focused on the geodetic receivers only, which will be the ones used for the experiments in the next chapters. Besides the hardware, the chapter also presented different geodetic approaches that can be used to collect data and post-processing it, generating the wanted local estimated clocks.

Chapter 4

PPP Time Transfer Using GAPS

This chapter provides an overview of GPS Analysis and Positioning Software (GAPS) software suite and its capability for being used as a tool for time and frequency analysis. GAPS is a PPP software initially developed for positioning, but quickly it showed its capability to be used for data analysis.

The next sections in this chapter will show the main changes and updates made in GAPS, to build capabilities to be used as a timing tool. We are referring to GAPS with time transfer capabilities as GAPSTFT (GPS Analysis and Positioning Software for Time and Frequency Transfer). Also, GAPSTFT will includes an interface and some tools to operate phase and frequency data.

4.1 GAPS Algorithm

GAPS was developed at UNB initially by Leandro [2009], and has been under constant enhancements since then. GAPS algorithms and code structure follows some of the standards of GPS PPP approaches, but with some differences.

GAPS source code is mainly written in *Matlab*® program language. It is available as a free online service at the following address http://gaps.gge.unb.ca. The online version provides all the estimated values as output file, but its functionality is mostly focused on positioning users.

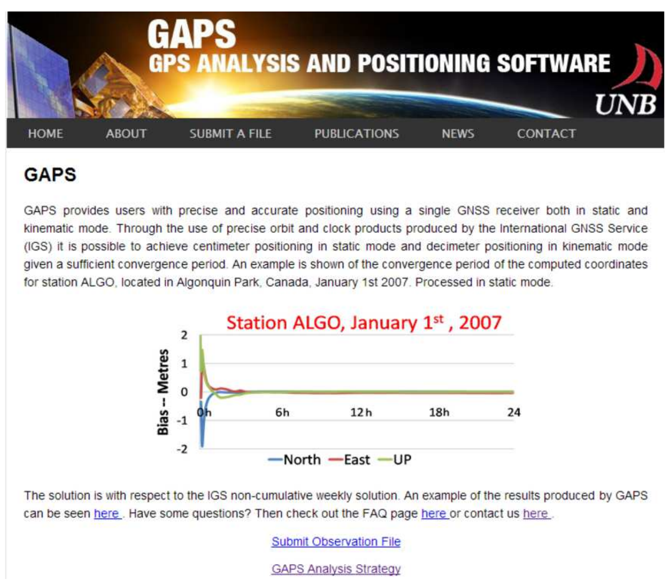

Figure 4.1: GAPS online main page

GAPS PPP approach is based on post-processing GPS observations collected by a single station, using the IGS final products and modeled ionospheric delays. Processing the dual frequency pseudorange and carrier phase observations and using models for all the physical phenomena involved, GAPS can achieve the precision of a few centimeters in horizontal coordinates and less than 10 cm in vertical coordinates.

Below is presented some of the main characteristics of how GAPS handles the estimation process:

- **Ionosphere:** Fist-order ionospheric delay is Eliminated by dual-frequency observations in a linear combination using carrier-phase measurements. Only first order ionospheric delay is modeled.

- **Phase rotation correction:** Satellite antenna phase wind-up is applied according to [Lichten et al., 1993].

- **Satellite antenna phase center correction:** Modeled using block-specific nadir angle-dependent. Absolute PCV values applied from the file $igsyy_w ww.atx$ and azimuth corrections. This file is an external input file which contains the absolute IGS phase center corrections for satellite and receiver antennas.

- **Satellite differential code bias:** Correction to P1 and P2 using monthly P1-C1 DCB solution provided by CODE and applied based on receiver type as given in *p1c1bias.hist*. This file is an external input file which contains the history of average P1-C1 biases values recommended by the IGS for its Analysis Centers and for users of IGS products.

- **Satellite center-of-mass offset:** offset treated using information from manufacturers contained in file $igsyy_w www.atx$, based on GFZ/-TUM analysis fixed to ITRF2008.

- **Receiver antenna phase center correction:** Absolute and elevation and azimuth-dependent (when available). PCV values obtained from file the external input $igs08_w www.atx$, provided by the IGS.

- **Receiver antenna phase center offset:** L1/L2 offsets applied from the external input file $igs08_w www.atx$, provided by the IGS.

- **Tidal displacements:** At the beginning of this work, the only tidal displacement used by GAPS was the Solid Earth tide based on IERS 2003 conventions. The next sections will present the new tide displacements corrections implemented on GAPS.

- **Relativistic effects:** Based on the gravitational time delay [Kouba, 2009].

- **Adjustment:** Sequential least squares with weighted constraints is used to estimate the unknown parameters.

- **Station coordinates:** Either estimated, held fixed or constrained.

- **Receiver clock estimation:** Modeled as white noise with a large value to handle the clock resets.

- **Troposphere estimation:** Estimated for each observed epoch as a random walk with a default process noise of $5mm/sqrt(hr)$. The mapping function used is the VMF1 (gridded). The gradients are estimated for each observation as a random walk following [Chen and Herring, 1997].

- **Ambiguity:** Estimated as real numbers.

- **Precise IGS orbit products:** IGS orbit final products with 15 min interval are used. The orbit interpolation is done with the adjustment of a 16^{th} degree polynomial fitted to 6h-long arc.

- **Precise IGS clock products:** IGS clock final products with 5 minute interval are used. The clock interpolation is done with the adjustment of a 2^{nd} degree polynomial for every 20 min arc, for each satellite.

More details about GAPS PPP approach can be found in Leandro [2009].

4.2 Time Specific Improvements

For the purpose of using and testing GAPS as a tool for time purpose and clocks comparison, some updates were made to GAPS. The following sections and subsections will present the implementation and updates.

4.2.1 Solid Earth Tides

The solid earth tide is a motion of the solid Earth's surface. This motion is caused mainly by the gravity of the Moon and Sun, over the Earth, and causes the displacement of reference points, such as GNSS stations.

The International Earth Rotation and Reference Systems Service (IERS) provides the mathematical models which describe the displacements of reference points. For this research, GAPS was updated to apply the solid Earth tides correction following the IERS 2010 conventions. More details about Earth tides can be found in the IERS 2010 conventions technical notes [Petit and Luzum, 2010].

4.2.2 Ocean Tide Loading

Ocean tides result in a temporal variation of the ocean mass distribution and load on the crust and produce time-varying deformations on the Earth that can reach up to 100 mm, [Petit et al., 2010]. This effect is mainly also due to the gravitational attraction of the Moon and the Sun. As with the solid the Earth's tide, the ocean tide loading (OTL) causes sites displacements on Earth's surface.

The displacement and magnitude values depend on the site location and the period of the day. The displacements can be obtained following the IERS 2010 Conventions model. The model needs as an input information, the site-dependent tidal coefficients, which are provided the Ocean Loading Service

(OLS) website, http://holt.oso.chalmers.se/loading/ [Scherneck et al., 1998].

The OTL requires input information to provide the correct coefficients according to the user is need. Below you can find the list of input information required:

- **Models:** It provides a list of ocean tide models available, for instance: $GOT00.2$ and $FES2004$

- **Type of loading phenomenon:** vertical and horizontal displacements or gravity

- **Coordinates:** the site coordinates must be provided in geodetic or Cartesian coordinates

- **Output formats:** there is a choice between two output files format: BLQ and HARPOS

Figure 4.2 shows as an example the OTL displacements calculated by GAPS to be applied during its PPP estimation process.

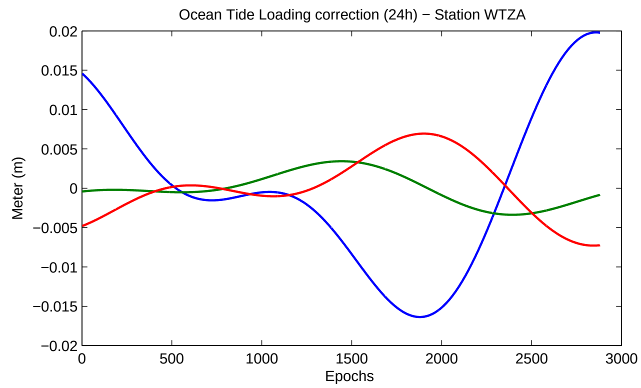

Figure 4.2: OTL displacements for station WTZA

4.2.3 Accepting IGS Rapid products

The basic concept of PPP is to use the IGS precise products during the estimation process. As explained before, these products, made available by the IGS, are the GNSS satellite ephemerids/clocks and station clocks. The products are available in different accuracies and latencies, see Table 4.1.

Table 4.1: IGS Product Table

Products		Accuracy	Latency	Interval
Broadcast	orbits	100 cm	real time	daily
	Sat. clocks	5 ns RMS 2.5 ns SDev		
Ultra-Rapid	orbits	5 cm	real time	15 min
	Sat. clocks	3 ns RMS 1.5 ns SDev		
Ultra-Rapid	orbits	3 cm	3-9 hours	15 min
	Sat. clocks	150 ps RMS 50 ps SDev		
Rapid	orbits	2.5 cm	17-41 hours	15 min
	Sat. & Stn. clocks	75 ps RMS 25 ps SDev		5 min
Final	orbits	2.5 cm	12-18 days	15 min
	Sat. & Stn. clocks	75 ps RMS 20 ps SDev		Sat.: 30s Stn.: 5 min

So far GAPS took advantage only of the IGS final products. These products have the best accuracy to both satellite orbits and clock, however the latency of these products is about 12 to 18 days. Thanks to the improvements made by IGS to the rapid products accuracy, we have now the rapid products achieving accuracy similar to those of as the final products, but with a shorter latency of only 14 to 41 hours.

To be able to process observation files collected within two days, instead of one week, GAPS was updated to accept the IGS rapid products as input. GAPS will check first if the final products are available, in case they are not, the rapid products will be used.

4.2.4 Internal Delays

Most of the geodetic GNSS receiver models used for timing purpose do not apply the internal delays (equation 3.1) to the RINEX data files. That happens because those receivers were developed for geodetic purpose, which the absolute values are not needed.

GAPS has been adapted to apply the total internal delays to its estimated clocks. A list of known internal delays for timing stations was added to GAPS data base, and a list of them is presented in Table 4.2.

Table 4.2: Stations contributing for TAI using PPP method

Station	Receiver's name	Calibration	Receiver Type	Reference
AOS	ao-4	Manufacturer	TTS-4	UTC(AOS)
BEV	be1-	Manufacturer	TTS-4	UTC(BEV)
DLR	obet	BIPM-trip	Sept. PolaRx2	UTC(DLR)
DMDM	dmdm	Manufacturer	GTR50	UTC(DMDM)
DTAG	dt01	Manufacturer	Dicom GTR-50	UTC(DTAG)
ESOC	estc	Indirect	Sept. PolaRx3eTR	UTC(ESTC)
HKO	hko1	Manufacturer	TTS-4	UTC(HKO)
IFAG	wtza	BIPM-trip	Ashtech Z-XII3T	UTC(IFAG)
GUM	gum4	Manufacturer	TTS-4	UTC(PL)
INRiM	ieng	BIPM-trip	Ashtech Z-XII3T	UTC(IT)
IPQ	ip02	Manufacturer	TTS-4	UTC(IPQ)
KRISS	kris	BIPM-trip	Ashtech Z-XII3T	UTC(KRIS)
METAS	wab2	BIPM-trip	Ashtech Z-XII	UTC(CH)
MIKES	migt	Manufacturer	Dicom GTR-50	UTC(MIKE)
NICT	sepb	Indirect	Sept. PolaRx2TR	UTC(NICT)
NIM	imej	BIPM-trip	JPS EUROCARD	UTC(NIM)
NIST	nist	None	Novatel OEM4	UTC(NIST)
NMIA	sydn	BIPM-trip	Javad Euro-160	UTC(AUS)
NMIJ	nm0c	BIPM-trip	Ashtech Z-XII3T	UTC(NMIJ)
NPL	np11	Manufacturer	Dicom GTR-50	UTC(NPL)
NRC	nrc3	BIPM-trip	Ashtech Z-XII3T	Maser
NRL	nrl1	Absolute	Ashtech Z-XII3T	UTC(NRL)
ONRJ	rjep	BIPM-trip	Sept. PolaRx2e	HP 5071A
OP	opmt	BIPM-trip	Ashtech Z-XII3T	Maser
ORB	brux	Indirect	Sept. PolaRx4	UTC(ORB)
PTB	ptbb	BIPM-trip	Ashtech Z-XII3T	UTC(PTB)
ROA	roap	Indirect	Sept. PolaRx3TR	UTC(ROA)
SG	sg2p	BIPM-trip	Sept. PolaRx2	UTC(SG)
SMD	smbd	Manufacturer	TTS-4	UTC(SMD)
SP	sp01	BIPM-trip	Javad LGGD	UTC(SP)
TCC	cont	BIPM-trip	Sept. PolaRx2	Maser EFOS
TL	twtf	BIPM-trip	Ashtech Z-XII3T	UTC(TL)
TP	tp04	BIPM-trip	Dicom GTR-50	UTC(TP)
USNO	usn6	none	Novatel OEMV3	UTC(USNO)
VSL	vsle	none	Sept. PolaRx2	UTC(VSL)

4.2.5 Day Boundary Discontinuities

As mentioned before, the IGS products are made available in daily solution files. Processing through two consecutive days causes a discontinuity of the phase ambiguities through the midnight epoch, from one day to the following one, resulting in a high uncertainty between two consecutive days [Matsakis et al., 2006; and Dach et al., 2005].

Computing daily independent files using PPP, makes it estimated solutions to have what is called "day boundary discontinuities" (DBD). For this work in specific, we are concerning about the jumps caused by the DBD in the estimated clocks over midnight, which can reach the magnitude of approximately 1 ns.

Another problem related to the DBD is the convergence time that every day solution will present in the PPP estimated parameters. Figure 4.3 shows the DBD effects (spikes) in the estimated clock.

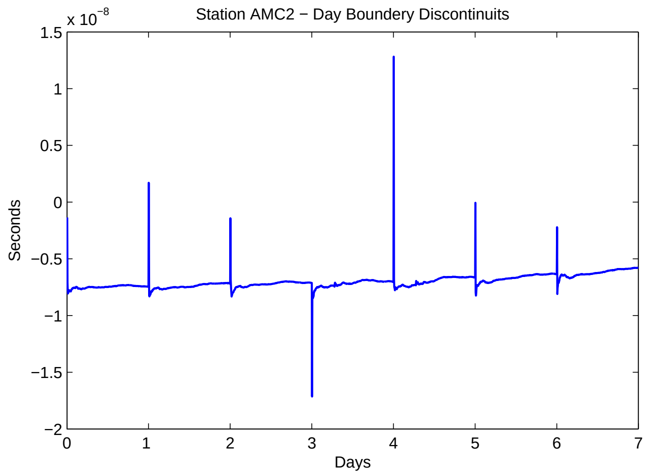

Figure 4.3: PPP solutions showing the DBD effect on the clock estimation

Since any GNSS receiver can work over midnight and so do the clocks, there is no hardware reason to have a DBD in the geodetic time and transfer solutions. Trying to connect the daily independent solutions over many days using PPP, some researchers have proposed methods to solve this problem, see [Orgiazzi et al., 2005; Guyennon et al., 2009].

To solve the DBD issue, GAPS was enhanced to allow the use of processing information from the previous day as input for the following day. This modification allows to propagate the covariance information from day $i-1$ to day i, where the $C_{\hat{X}_{i-1}}$ has to be updated to include process noise represented by the covariance $C\varepsilon_{\Delta t}$. By the end, we have the variable $P_{X_i^0}$ carrying the information from the previous day to the following one:

$$P_{X_i^0} = [C_{X_{i-1}^{\hat{}}} + C\varepsilon_{\Delta t}]^{-1}, \tag{4.1}$$

where

$$C\varepsilon_{\Delta t} = \begin{bmatrix} C\varepsilon(x)_{\Delta t} & 0 & 0 & 0 & 0 & 0 \\ 0 & C\varepsilon(y)_{\Delta t} & 0 & 0 & 0 & 0 \\ 0 & 0 & C\varepsilon(z)_{\Delta t} & 0 & 0 & 0 \\ 0 & 0 & 0 & C\varepsilon(dT)_{\Delta t} & 0 & 0 \\ 0 & 0 & 0 & 0 & C\varepsilon(zpd)_{\Delta t} & 0 \\ 0 & 0 & 0 & 0 & 0 & C\varepsilon(N)_{\Delta t} \end{bmatrix}$$

It is known that the receiver clock process noise can change as a function of frequency stability, so it is set to white noise with a large value to handle the unpredictable clock resets. The method implemented to reduce the DBD using the continuation of the Px matrix will be called as multi-day continuous processing mode.

Figure 4.4 show an example of the multi-day continuous processing reducing the DBD for the station AMC2.

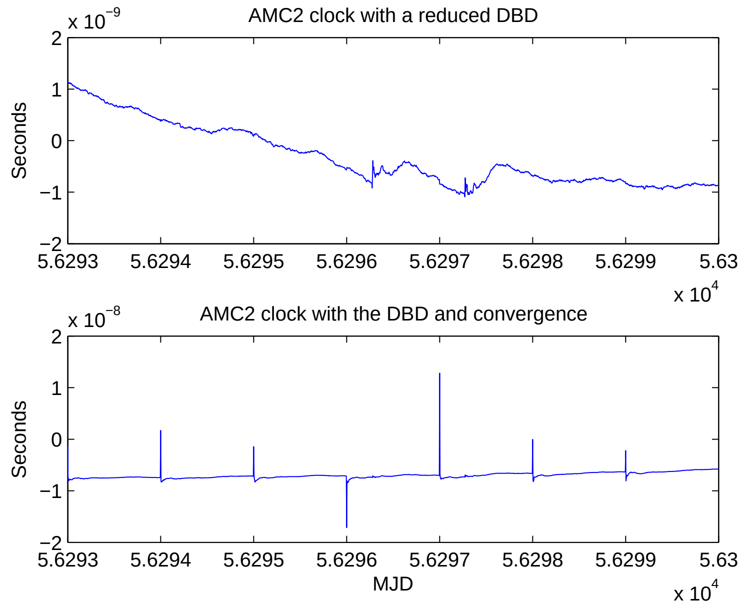

Figure 4.4: Comparison between AMC2 estimated clocks with DBD and DBD reduced by propagating the $P_{X_i^0}$ through consecutive days

4.3 GAPSTFT: implementations and add-ons tools for analysis of time and frequency stability

The original GAPS software is available to the public only in an online version. This version accepts just one file with 24 hours maximum of observations each submission. For time and frequency transfer purpose is often necessary to process more than 30 days of data using the multi-day continuous processing mode mentioned before in this Chapter. Uploading a huge number of observation files online for many stations would not be a productive way of working. For this reason, GAPSTFT has been implemented to run as an Desktop software. Also, an interface was developed for GAPSTFT, making the software more user friendly.

The process of estimating the clocks, processing a time and/or frequency link, and then do the analysis of the time and frequency stability, can be a long process prone of mistakes while manipulating the files. Also, different software suites are requested to process all the results that are needed. That being said, GAPSTFT was designed to be able to provide the most important information for those who work with time and frequency transfer.

4.3.1 GAPSTFT: implementations and add-ons for time and frequency analysis

In this subsection, we present GAPSTFT's interface developed to accommodate the time implementations presented in the section 4.3, and also the new tools (add-ons) to perform a time and frequency analysis.

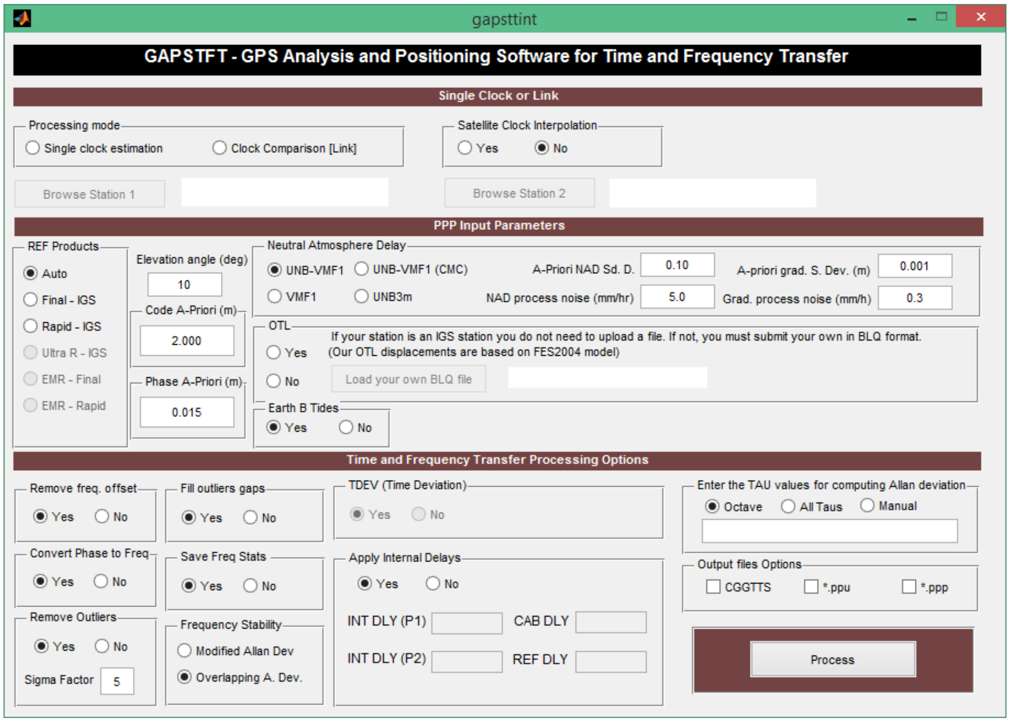

Figure 4.5: GAPSTFT Interface

The processing options in GAPSTFT were organized in three processing mode groups: *(1) Single clock or link, (2) PPP Input Parameters and (3) Time and Frequency Options*. Each option will be explain in this section.

1. Single clock or link

This group presents the following add-ons to GAPS:

- **Single clock estimation:** estimates the receiver clock for one single station with reference to one of the input products (e.g.,IGS Final, IGS Rapid). This option is able to perform a multi-day continuous processing up to a period of one year.

- **Clock comparison (link):** estimates clocks of two chosen stations, using the principles of all-in-view method. The time and frequency link between the two station is performed. This option is able to perform a multi-day continuous processing up to a period of one year.

- **Satellite clock interpolation:** When the product is not available at the rate of 30 seconds, GAPSTFT can interpolate the input offsets clock for to watch that rate.

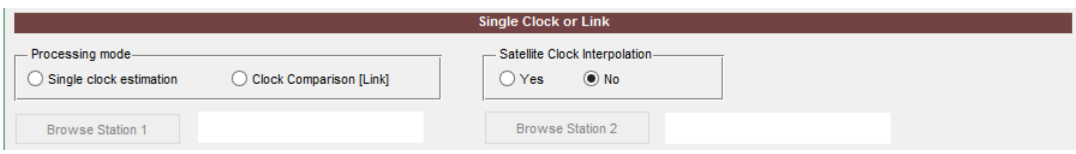

Figure 4.6: Single clock or Link options

2. PPP Input Parameters

In this second group, all add-ons are related to the PPP processing parameters:

- **REF Products:** allows the user to select which kind of product (e.g., IGS Final, IGS Rapid) be used as reference for the station estimated clocks.

- **Elevation angle:** allows the user to input the elevation angle cutoff in degrees

- **Code A-Priori sigma (m):** allows the user to set an a-priori std for the code measurements.
- **Phase A-Priori sigma (m):** allows the user to set an a-priori std for the phase measurement.
- **Neutral Atmospheric delay:** offers to the user four different troposphere models. Also, the parameters for the modeling can be set by the user.
- **Earth Body Tides:** the body tide corrections can be selected.
- **Ocean tide loading:** the ocean tide corrections can be selected. The user also has the option to input their own file with the corrections.

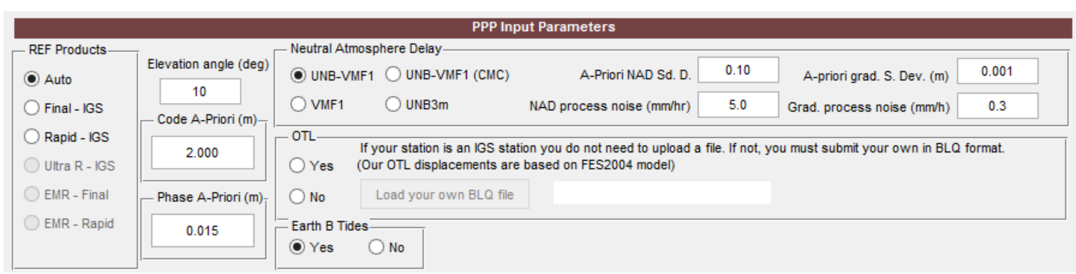

Figure 4.7: PPP Input Parameters

3. Time and Frequency Transfer Processing Option

The third and last group of add-ons presents the implementations related to time and frequency analysis.

The developments and implementation discussed next follow guidelines according to Riley [2003].

It is essential that the clock-phase data are an array with equally-spaced phase or frequency values. The data also must have a time tag associated with it. Usually, the mostly used time tag is the Modified Julian Date (MJD). It is also preferable that all the data is stored as numerical ASCII file.

GAPSTFT provides directly the estimated clock-phase, but for time and frequency transfer, it is very important the conversion of the phase data to frequency.

Once we have the clock-phase and frequency stored in a proper way, we can start to do the data analyses. The visual analysis of time and frequency is very important. The visible outliers must be removed from the data, and so the drift and frequency offset. The outliers and other gaps in the data must be replaced before the frequency stability analysis.

Based on the previous information about how to handle the time and frequency analysis, GAPSTFT was updated to handle the time and frequency analysis in an easy and automatic way:

- **Phase data:** after the PPP processing, the estimated clock phase are stored in a file, with extension *.clk3 and MJD time tag.

- **Convert Phase to Frequency:** Phase data is converted to frequency by dividing the difference between the two consecutive phases by the sampling rate τ:

$$y_i = (x_i - x_{i-1})/\tau, \tag{4.2}$$

where y_i is the frequency value at epoch i, x_i is the clock phase value at the same epoch and x_{i-1} is the clock phase at the previous epoch.

- **Remove drift:** Remove the drift from receiver clock offset time series using a least squares quadratic fit, [Riley, 2008].

$$d(t) = a + bt + ct^2 \tag{4.3}$$

for $y(t) = d'(t) = b + 2ct$, slope $d'(t) = 2c$, where a, b and c are the coefficients, having units of sec, sec/sec, and sec/sec^2, respectively, and the frequency drift slope and intercept are $2c$ and b, respectively.

- **Remove outliers:**Remove the outliers following the median absolute deviation (MAD). The median absolute deviation can be defined as the median of the scaled absolute deviations of the data points from their median value:

$$MAD = Median\{|y(i) - m|/0.6746\} \tag{4.4}$$

where m is the Median $\{y(i)\}$, $y(i)$ is each frequency data point and m is the median value of the data set. In this analysis, each frequency data point is compared with the median value of the data set, and then subtracted or summed from/to the desired multiple of the MAD.

- **Fill outliers gaps:** gaps are filled with the interpolated values from the array.

- **Save freq statistics:** it stores statistical information from the frequency.

- **Frequency stability:** this option provides a tool for a measure of time-domain frequency stability. For this version of GAPSTFT, only the Overlapping Allan deviation option has been implemented following the equations by [Riley, 2007].

$$\sigma_y^2(\tau) = \frac{1}{2m^2(M-2m+1)} \sum_{j=1}^{M-2m+1} \{ \sum_{i=j}^{j+m-1} [y_{i+m} + y_i] \}^2 \tag{4.5}$$

  The Overlapping Allan Variance $\sigma_y^2(\tau)$ can be calculated when $\tau = m\tau_0$ is averaging time, m is the averaging factor, τ_0 is the basic measurement interval, y is the ith of M fractional frequency values.

- **TDEV (Time Deviation):** this tool provides the option to generate a time deviation analysis. In this version of GAPSTFT this option has not been implemented yet.

- **Apply Internal delays:** allows the user to enter the internal delay values for the station(s), following the equation 3.1.

- **Output file options:** allows the user to select an output file format options between: *CGGTTS* format, *ppu* format (clock phase without the internal delays) and *ppp* format (clock phase values with the applied internal delays).

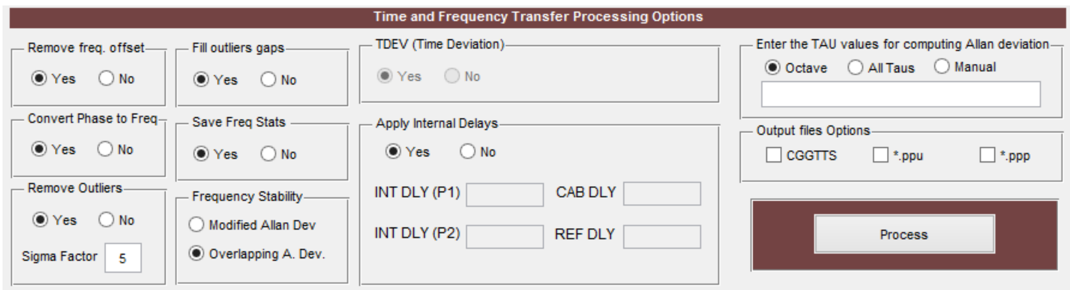

Figure 4.8: PPP Input Parameters

4.4 Summary

This chapter presented an overview of GAPS software algorithm based on its mathematical models and functionality. Also, we presented the main changes made in GAPS source to make it a time and frequency tool. The implementations to automatize the process of getting the estimated clocks and providing a time and frequency stability analysis were also provided in this Chapter.

Chapter 5

Experiments

In this chapter we describe the assessment of GAPSTFT. We first present the data used in the assessment, its availability and quality. In a second step, we present the results of the new implementations using different options and case scenarios. Following the results, we also present different ways of evaluating it through statistic values, instability of the clock phase and frequency, and comparisons with other software suites and method.

5.1 Selected IGS Timing Station and GNSS Data

For the experiments, fourteen worldwide stations from IGS were selected. Ten of them are also part of the BIPM TAIPPP project [Petit and Arias, 2009]. Table 5.1 presents the selected stations, their location and the type of atomic clock driving each station.

Table 5.1: List of chosen stations for the experiments

	City	**Country**	**Agency**	**Clock**
AMC2	Colorado Springs	U.S.A.	USNO	H-MASER
BREW	Brewster	U.S.A.	JPL	External H-MASER
BRUX	Brussels	Belgium	ROB	External 5071A CESIUM
IENG	Torino	Italy	I.N.RI.M.	External H-MASER
NIST	Boulder	USA	NIST	External H-MASER
NRC1	Ottawa	Canada	NRCan	H-MASER
ONSA	Onsala	Sweden	LMV	External H-MASER
OPMT	Paris	France	OP	External H-MASER
PTBB	Braunschweig	Germany	BKG	External External H-MASER
ROAP	San Fernando	Spain	ROA	External H-MASER
SYDN	Sydney	Australia	GA	External CESIUM
TWTF	Taoyuan	China	TL	External H-MASER
USN3	Washington	U.S.A.	USNO	H-MASER
WAB2	Wabern	Switzerland	METAS	External Master
WTZA	Bad Koetzting	Germany	BKG	CESIUM

The data campaign selected for the experiments corresponds to the period between January 31^{st}, 2012 and January 31^{st}, 2013. All the data are assembled from the daily RINEX files at 30 seconds sampling rate, making it a total of 434 RINEX files.

An evaluation was performed on the dataset, in search of missing daily files and lacking of a considered amount of observations in each RINEX. The results of this search are:

- No RINEX file was missing from any station during the campaign period.

- Five stations were unable to present seven consecutive days of data without missing a considerable amount of observations: BRUX, OPMT, TWTF, USN3 and WAB2. For this reason, these stations were left out of the experiments.

- Five stations presented some missing data, but not a considerable amount of data that would affected the experiments up to 5 months: AMC2, NIST, ONSA, USN3 and WAB2.

- Five stations have no considerable amount of missing data during thirty consecutive days: IENG, NRC1, PTBB, ROAP and WTZA.

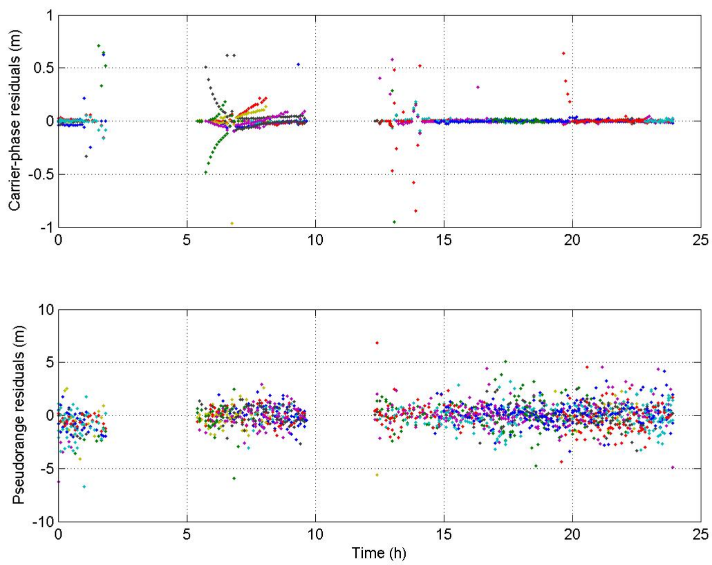

Figure 5.1: Effects of missing data on carrier phase and pseudorange residuals - Station NIST

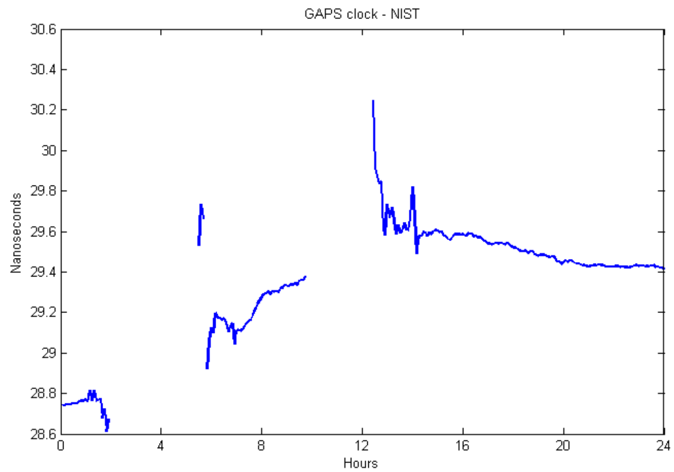

Figure 5.2: Effects of missing data on the estimated clocks

5.2 Multi-day continuous processing results

The first GAPSTFT implementation and assessment to be presented is the called "multi-day continuous processing option", which is intended to solve the day boundary discontinuities problem.

As discussed Chapter 4, the DBD was solved by passing along all the filter information from a previous day to the following one.

The multi-day continuous processing option initializes a new ambiguity solution every midnight, resulting on a new clock receiver estimation at the same time. On the other hand, multi-day continuous processing uses the estimated parameters from one day to the other, avoiding the ambiguity reseting problem. Below you can see figures and statistics comparisons between the day-by-day and multi-day continuous processing.

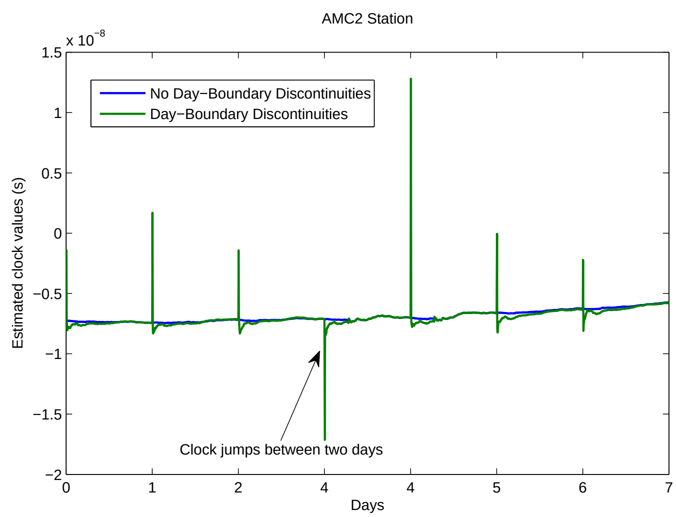

Figure 5.3: Comparison between day-by-day and multi-day continuous processing

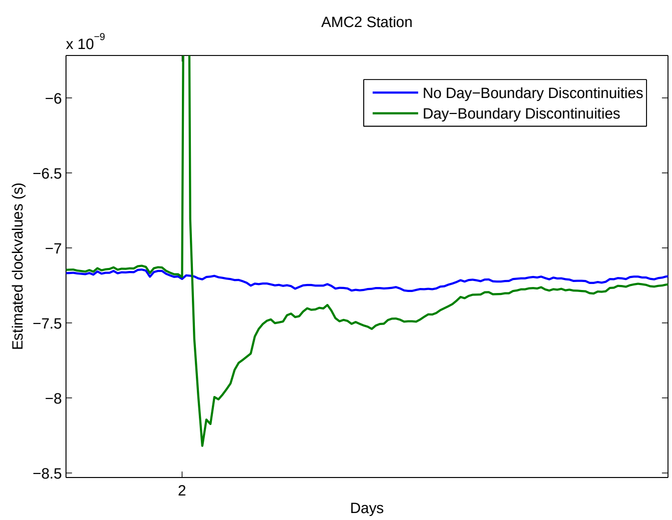

Figure 5.4: Comparison between day-by-day and multi-day continuous processing (zoom in)

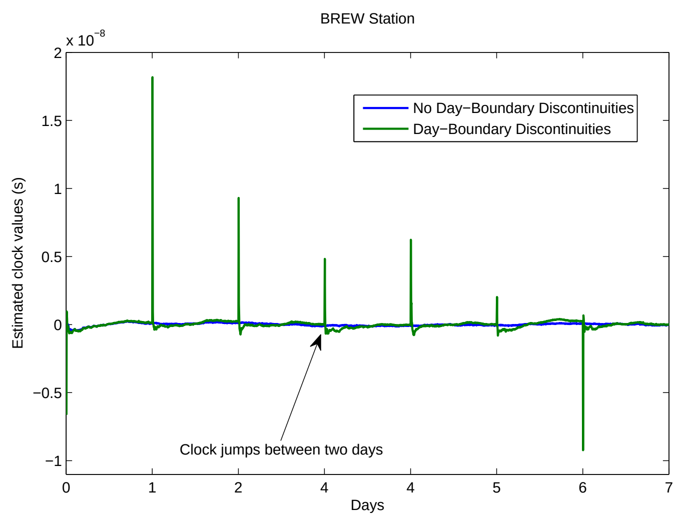

Figure 5.5: Comparison between day-by-day and multi-day continuous processing

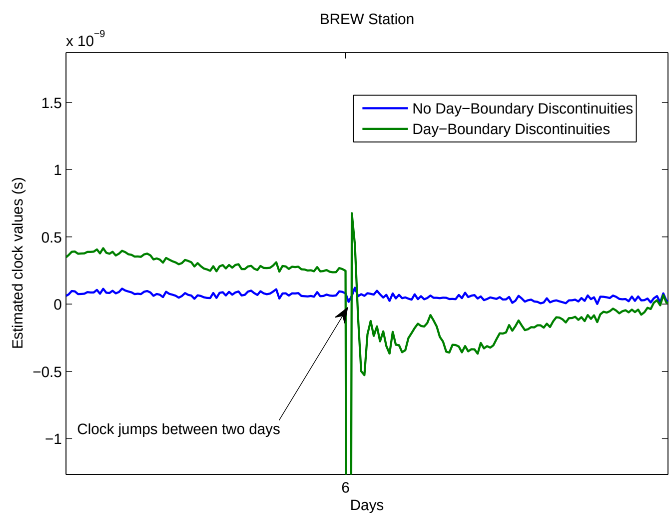

Figure 5.6: Comparison between day-by-day and multi-day continuous processing (zoom in)

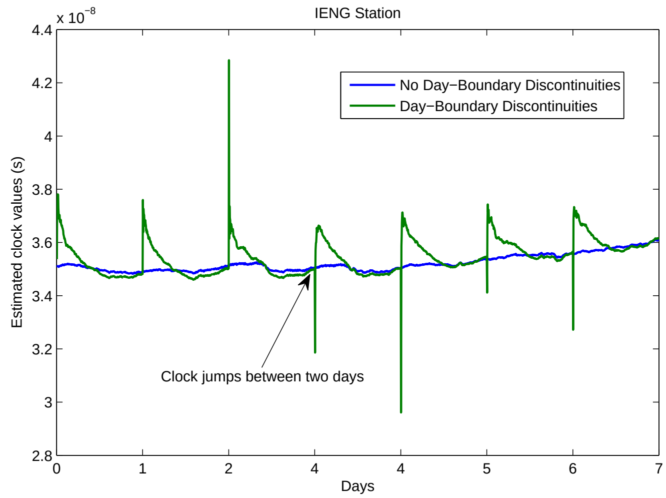

Figure 5.7: Comparison between day-by-day and multi-day continuous processing

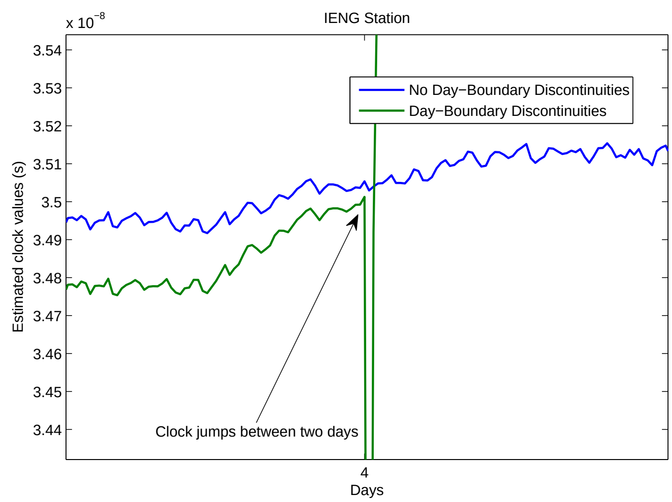

Figure 5.8: Comparison between day-by-day and multi-day continuous processing (zoom in)

Table 5.2: Comparison between day-by-day (DBD) and multi-day continuous processing (MDC) (values in seconds).

		Max Value	**Min Value**	**Mean**	**median**	**STD**
AMC2	*MDC*	-5.72E-09	-7.46E-09	-6.90E-09	-7.09E-09	4.66E-10
	DBD	1.28E-08	-1.71E-08	-7.00E-09	-7.11E-09	7.71E-10
BREW	*MDC*	2.57E-10	-4.83E-10	7.90E-11	6.64E-12	1.05E-10
	DBD	1.81E-08	-9.22E-09	1.90E-10	-7.89E-13	5.94E-10
IENG	*MDC*	3.61E-08	3.48E-08	3.52E-08	3.51E-08	3.14E-10
	DBD	4.28E-08	2.96E-08	3.54E-08	3.53E-08	6.55E-10

Table 5.2 shows that the MDC processing can be 2 (Station IENG) to 6 (Station BREW) times better regarding the standard deviation of the final clock estimation, and, therefore, we expect it to achieve a better frequency stability (i.e., smaller ratio) for the final estimation. From those results, we can conclude that the MDC implementation was successful and will play an important role for GAPSTFT in the way to become a suitable time and frequency transfer software. The following experiments will use this new implementation as a standard.

5.3 Implementation of GAPSTFT to support IGRT products

According to IGS service, the "rapid" products are being offered with the same accuracy than the "final" products. However, the rapid products have a shorter latency, making it available to users much faster than the final ones. The final products are available at 12 days latency, while the rapid products are available with approximately 17 hours .

Corresponding to each of the rapid and final IGS clock products, we name IGRT as rapid product timescale and IGST as final product timescale. The plots below show the comparison between the estimated clocks using IGRT and IGST for station AMC2, PTBB and IENG.

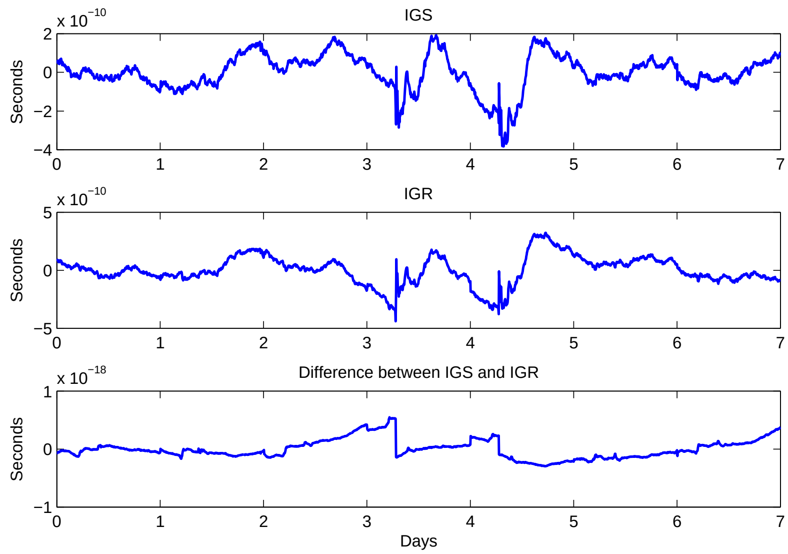

Figure 5.9: Comparison between estimated clocks referenced to IGST and IGRT - station AMC2.

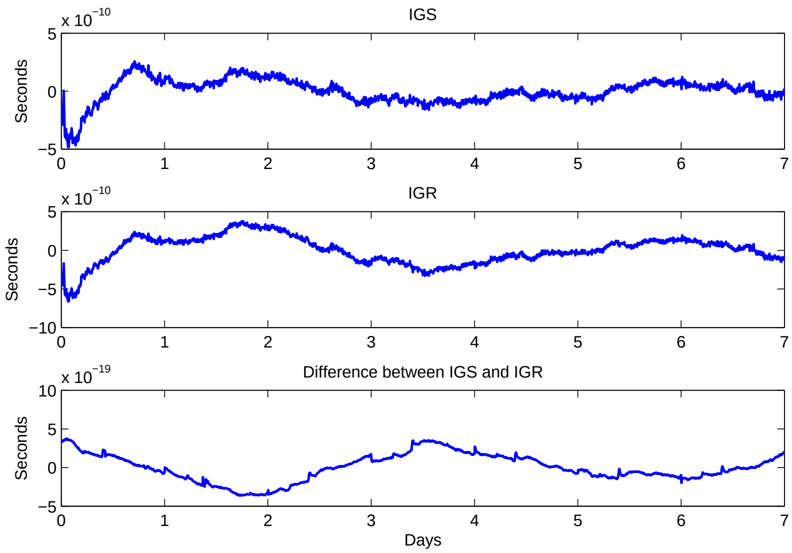

Figure 5.10: Comparison between estimated clocks referenced to IGST and IGRT - station PTBB.

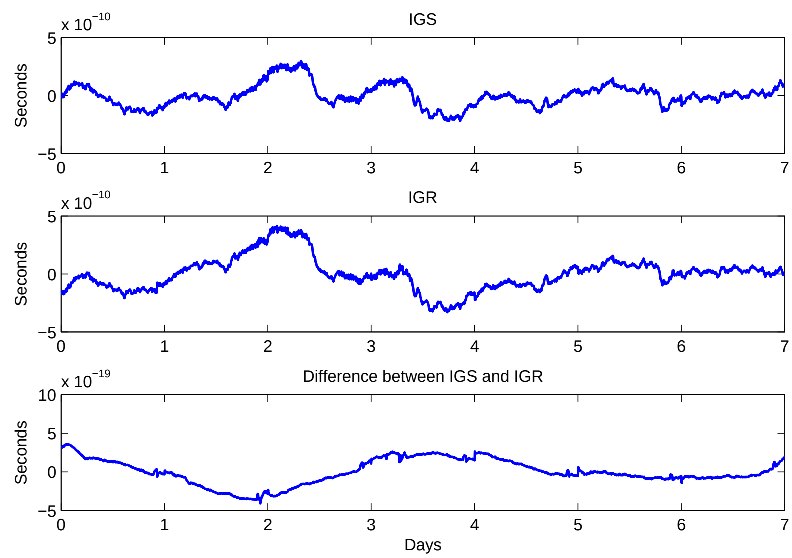

Figure 5.11: Comparison between estimated clocks referenced to IGST and IGRT - station IENG.

Figures 5.10 and 5.11 show us a good agreement between the clocks estimated using IGRT and IGST. The difference between the two results shows values of magnitude of 10^{-19}, which makes the two results for time and frequency transfer compatible.

The benefit of this implementation will allow the time and frequency users to run GAPSTFT and get clock estimated values as soon as 17 hours after collecting their GPS observations.

5.4 GAPSTFT: single clock estimation option

In this section we will present the results provided by GAPSTFT using the *single clock estimation* (cf. Section 4.3.1) mode, followed by a comparison between results using 30 seconds rate and 5 minutes rate. Also, an evaluation of the short and long term clock estimation will be shown.

5.4.1 Five minutes and thirty seconds rate clock estimation

To get the clock estimated solution in this section, a campaign of 7-days of observation for each station was selected. The processing mode was based on the called *multi-day continuous processing*, eliminating the day boundary discontinuities.

The selected stations for this experiment are: AMC2, BREW, IENG, NRC1, ONSA, PTBB, ROAP, USN3 and WTZA.

Below we show the PPP input parameters used to perform the estimation.

- REF products: **IGS Final**
- Elevation Angle: **10 degrees**
- Earth Tides: **Yes**
- Ocean tide Loading: **Yes**; **FES2004 model**
- Neutral Atmosphere Delay: **VMF1**; A-Priori NAD: **0.10**; NAD process noise (mm/hr): **5.0**; A-Priori grad S. Dev (m): **0.001**; Grad. process noise (mm/hr): **0.3**

We present statistic values showing a comparison between the clock solution for 5-min and 30-sec.

Table 5.3: Statistics values for all the nine selected station comparing the 5 min and 30 sec clock estimation

		Max (s)	**Min (s)**	**Mean (s)**	**Median (s)**	**std (s)**	**rms(s)**
AMC2	*5 min*	-5.722E-09	-7.461E-09	-6.908E-09	-7.096E-09	4.669E-10	9.894E-09
	30 s	-5.829E-09	-7.663E-09	-6.907E-09	-7.269E-09	4.734E-10	9.925E-09
BREW	*5 min*	2.575E-10	-4.830E-10	7.905E-11	6.643E-12	1.054E-10	4.748E-09
	30 s	2.835E-10	-4.878E-10	7.971E-11	6.780E-12	1.350E-10	4.983E-09
IENG	*5 min*	3.617E-08	3.438E-08	3.524E-08	3.512E-08	3.143E-10	2.58E-09
	30 s	3.76E2-08	3.841E-08	3.808E-08	3.943E-08	3.883E-10	2.794E-09
NRC1	*5 min*	-1.062E-09	-1.098E-09	-1.084E-09	-1.117E-09	8.400E-09	1.082E-08
	30 s	-1.087E-09	-1.119E-09	-1.094E-09	-1.125E-09	8.431E-09	1.137E-08
ONSA	*5 min*	6.847E-09	6.541E-09	6.694E-09	6.693E-09	8.875E-09	6.694E-09
	30 s	6.848E-09	6.540E-09	6.694E-09	6.693E-09	8.879E-09	6.694E-09
PTBB	*5 min*	5.087E-07	5.060E-07	5.068E-07	5.062E-07	8.791E-10	5.068E-08
	30 s	5.089E-07	5.028E-07	5.064E-07	5.060E-07	9.292E-10	5.064E-08
ROAP	*5 min*	-5.445E-08	-5.673E-08	-5.553E-08	-5.566E-08	6.603E-10	5.553E-08
	30 s	-5.352E-08	-5.794E-08	-5.572E-08	-5.582E-08	6.921E-10	5.572E-08
USN3	*5 min*	1.796E-09	-8.393E-10	3.560E-10	1.171E-10	6.278E-10	9.916E-09
	30 s	3.158E-09	-9.661E-09	2.231E-10	3.069E-11	8.156E-10	8.456E-10
WTZA	*5 min*	3.567E-07	3.502E-07	3.537E-07	3.538E-08	1.161E-09	3.537E-08
	30 s	3.577E-07	3.499E-07	3.587E-07	3.548E-07	1.177E-09	3.544E-08

Table 5.3 shows that both solutions, 5 minutes and 30 seconds, are compatible and preserve the same magnitude at each station for the two solutions. It is secure to say that GAPSTFT is ready and capable of providing time and frequency transfer solutions for both 5 minutes and 30 seconds clock rates.

This implementation will play an important role when it comes to frequency transfer. Estimating clocks at a higher rate allows the user to have more observations when calculating the frequency stability, which brings benefits to the frequency stability analysis of a station for a short term, such as 1 day.

5.4.2 Estimating clocks for short and long term

In this subsection, we present clock solutions based on 7-days, 30-days, 5-months and 1-year multi-day continuous processing. The idea is to present GAPSTFT capacity of estimating clocks for short and long periods. Then, an evaluation of the time and frequency stability will be presented.

The solutions were calculated based on the multi-day continuous processing eliminating the day-boundary-discontinuities, using the same PPP parameters used in the previous sub-section.

The chosen stations for the experiment in this subsection are AMC2, IENG, NIST, NRC1, ONSA, PTBB, ROAP, USN3, WAB2 and WTZA. Some stations such as NIST, present a considerable amount of gaps and outliers. The new GAPSTFT implemented tools for time and time transfer were used in this experiment. The drifts were removed from the clock solutions using the quadratic method. In this evaluation, the gaps from the phase-data were removed and filled with GAPSTFT tools. The outliers from the frequency were also removed and the gaps were filled.

Figures 5.12 and 5.13 show the estimated clocks for the ten selected stations for a period of one year. All of their drifts were removed, but ONSA and NRC1 because of their phase-clock jumps.

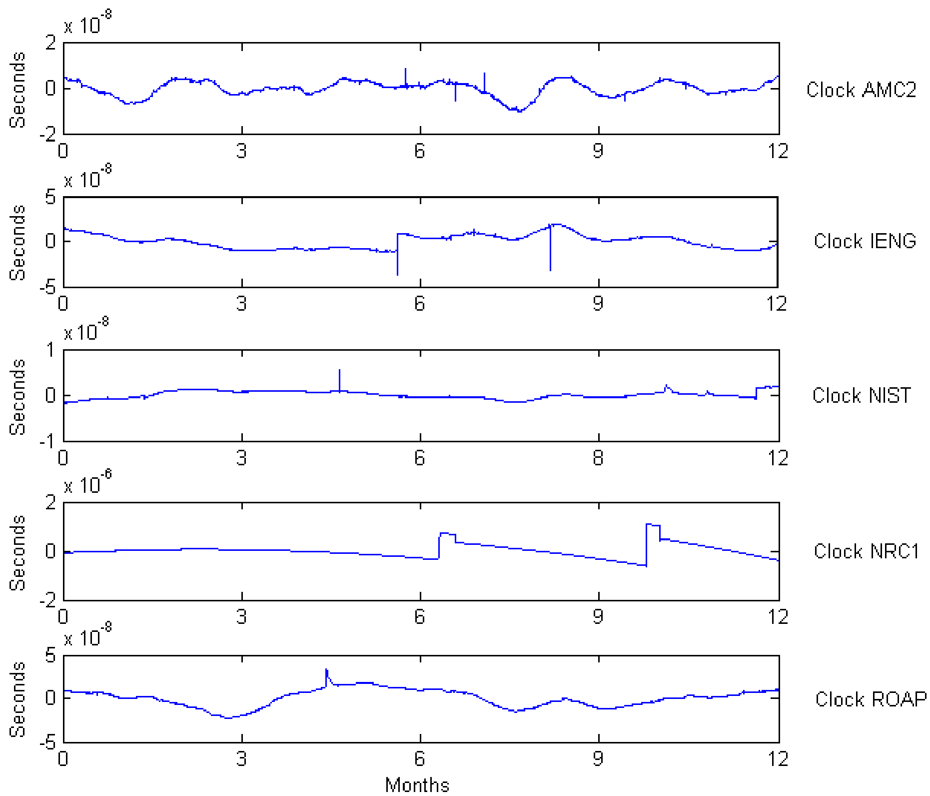

Figure 5.12: Estimated clocks by GAPSTFT for one year period

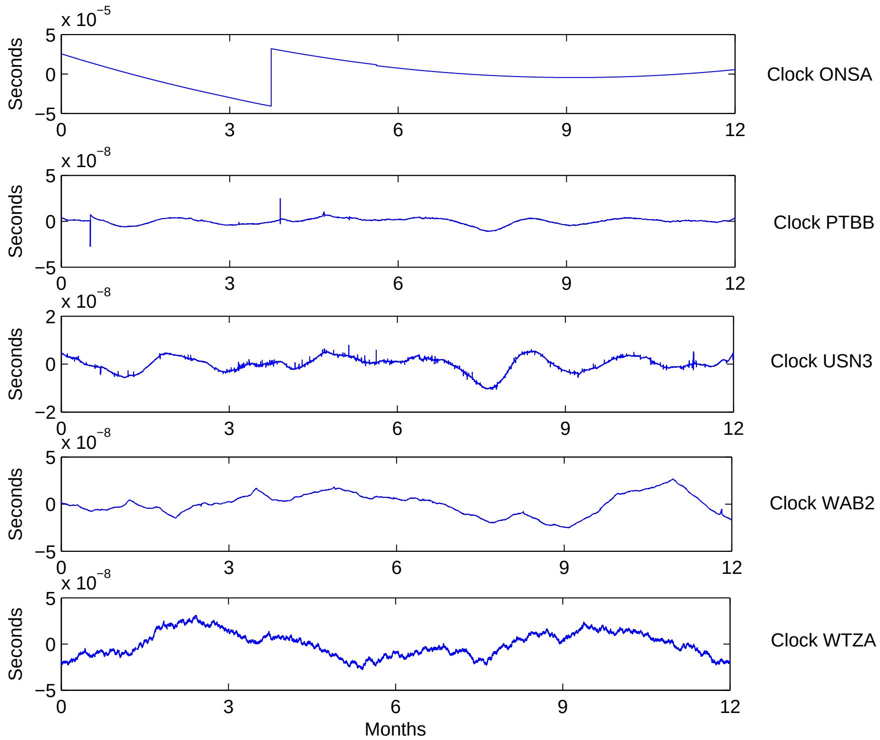

Figure 5.13: Estimated clocks by GAPSTFT for one year period

Even after eliminating most of the outliers from the clocks, we still can find some outliers and some jumps due to the missing data and ambiguity reset (station PTBB, Figure 5.13).

From the previous two figures, we can identify two stations (NRC1 and ONSA) presenting big jumps in their clock solutions, a behavior not considered a regular behavior for atomic clocks.

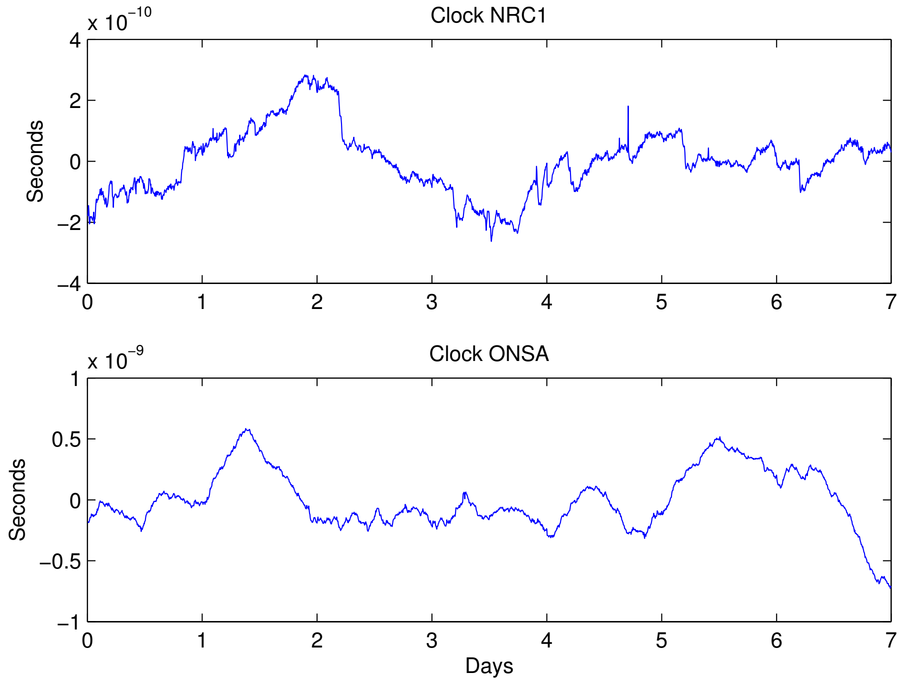

Figure 5.14: Example of 7-day processing with drift removed

Another way to evaluate the estimated clocks for short and long processing periods are to present the standard deviation and RMS values for the estimated clocks, see Table 5.4.

Expected standard deviation values for PPP estimated clocks range from 10^{-9} to 10^{-10}. Table 5.4 shows that most of stations, for short and long term estimation, present results within the expected range values. We can see an increase of the values, though proportionally, for longer periods of estimation.

As mentioned before, stations NRC1 and ONSA present an uncommon clock behavior and large jumps in the estimated clocks for a period of 1 year only, which brought the vales up to close to microsecond.

Table 5.4: Standard deviation (std) and rms of for the estimated clock phases for the period of 7 days, 30 days, 5 months and 1 year

		7 days	**30 days**	**5 months**	**1 year**
AMC2	*std (s)*	1.23E-10	4.28E-10	2.94E-09	3.27E-09
	rms (s)	1.23E-10	4.28E-10	2.94E-09	3.27E-09
IENG	*std (s)*	1.44E-10	4.44E-10	2.10E-09	7.84E-09
	rms (s)	1.44E-10	4.44E-10	2.10E-09	7.84E-09
NIST	*std (s)*	3.37E-10	3.96E-10	2.82E-09	7.81E-09
	rms (s)	3.37E-10	3.96E-10	2.82E-09	7.81E-09
NRC1	*std (s)*	1.06E-10	3.94E-10	3.31E-09	2.73E-07
	rms (s)	1.06E-10	3.94E-10	3.31E-09	2.73E-07
ONSA	*std (s)*	2.44E-10	3.99E-09	1.42E-05	1.52E-05
	rms (s)	2.44E-10	3.99E-09	1.42E-05	1.52E-05
PTBB	*std (s)*	1.34E-10	1.75E-09	2.75E-09	3.36E-09
	rms (s)	1.34E-10	1.75E-09	2.75E-09	3.36E-09
ROAP	*std (s)*	2.01E-10	8.63E-10	5.78E-09	1.00E-08
	rms (s)	2.01E-10	8.63E-10	5.78E-09	1.00E-08
USN3	*std (s)*	1.38E-10	4.21E-10	2.57E-09	3.14E-09
	rms (s)	1.38E-10	4.21E-10	2.57E-09	3.14E-09
WAB2	*std (s)*	2.30E-10	9.10E-10	4.03E-09	1.17E-08
	rms (s)	2.30E-10	9.10E-10	4.03E-09	1.17E-08
WTZA	*std (s)*	9.94E-10	2.15E-09	6.41E-09	1.32E-08
	rms (s)	9.94E-10	2.15E-09	6.41E-09	1.32E-08

GAPSTFT has been implemented to be used not only as a time transfer software, but also as a frequency transfer software. That being said, the next evaluation in this subsection will be testing GAPSTFT capability of performing frequency stability analysis for short and long periods of time.

The frequency stability analysis used the frequency data obtained from a conversion of the estimated clocks (clock phase) into frequency (section 4.3.1), using GAPSTFT new implemented tools. Table 5.5 shows GAPSTFT capacity of performing frequency stability analysis for short and long periods.

Table 5.5: Minimum overlapping Allan deviation (OADEV) values at the specif τ for each station for the periods of 7-days, 30-days, 5-months, 1-year

		7 days	**30 days**	**5 months**	**1 year**
AMC2	*OADEV*	2.71E-15	3.88E-15	5.07E-15	1.01E-15
	τ *(Sec)*	76800	122880	307200	4915200
IENG	*OADEV*	2.96E-15	2.00E-15	2.28E-15	2.12E-15
	τ *(Sec)*	76800	122880	307200	4915200
NIST	*OADEV*	5.49E-15	2.32E-15	2.95E-15	1.99E-15
	τ *(Sec)*	76800	122880	2457600	4915200
NRC1	*OADEV*	2.27E-15	1.73E-15	1.71E-15	1.25E-13
	τ *(Sec)*	76800	122880	153600	4915200
ONSA	*OADEV*	5.56E-15	2.86E-14	1.25E-11	7.18E-12
	τ *(Sec)*	76800	3840	2457600	4915200
PTBB	*OADEV*	2.82E-15	1.26E-14	3.06E-15	1.20E-15
	τ *(Sec)*	76800	122880	2457600	4915200
ROAP	*OADEV*	3.12E-15	3.33E-15	5.07E-15	4.52E-15
	τ *(Sec)*	38400	122880	1228800	4915200
USN3	*OADEV*	3.13E-15	4.41E-15	2.58E-15	1.02E-15
	τ *(Sec)*	76800	122880	307200	4915200
WAB2	*OADEV*	3.50E-15	4.05E-15	3.82E-15	4.10E-15
	τ *(Sec)*	76800	30720	2457600	4915200
WTZA	*OADEV*	2.40E-14	2.02E-14	7.12E-15	4.89E-15
	τ *(Sec)*	76800	122880	1228800	4915200

Table 5.5 shows that GAPSTFT can present good results in terms of frequency stability at the level of 10^{-15} for short and long term. Most stations are at this level. The other could have probably been driven to similar level, if as additional outlier removal was done, as it is the approach mostly used by time laboratories.

The frequency stability of the comparison between 7-day, 30-days, 5-months and 1-year periods, for some selected stations, can be shown in the next figures in terms of overlapping Allan deviation.

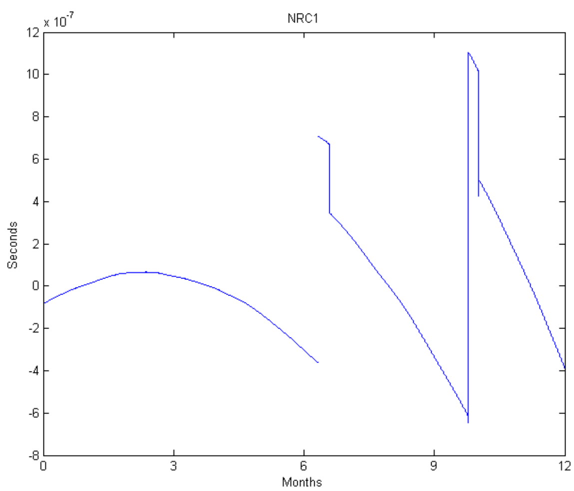

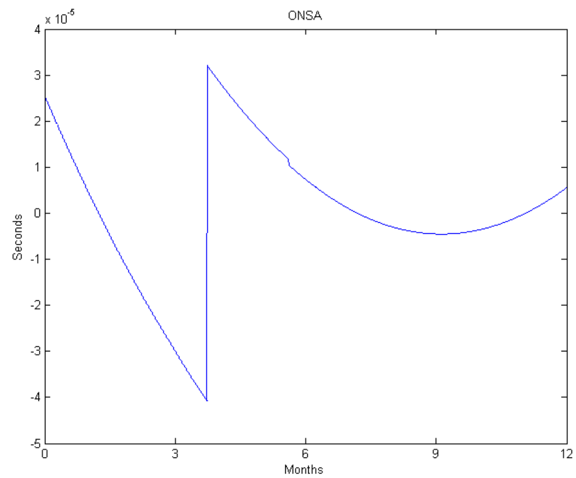

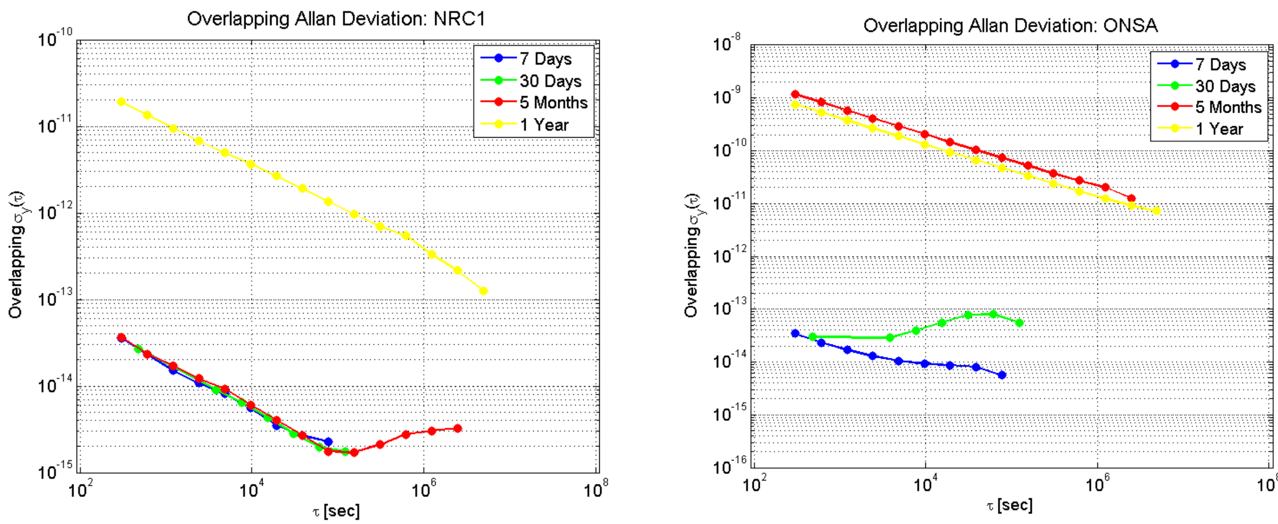

Figure 5.15: The two top figures show the estimated clocks for the stations NRC1 and ONSA. The two bottom figures shows the frequency stability respectively for the two stations

Figure 5.15 show how the jumps in the clock impacts on the frequency stability analysis, because they all should be very similar. In contrast to the stations NRC1 and ONSA, Figure 5.16 shows as an example the frequency stability the stations USN3 and WTZA, which presents closeness between the frequency stability calculated from short and long periods of clock estimation.

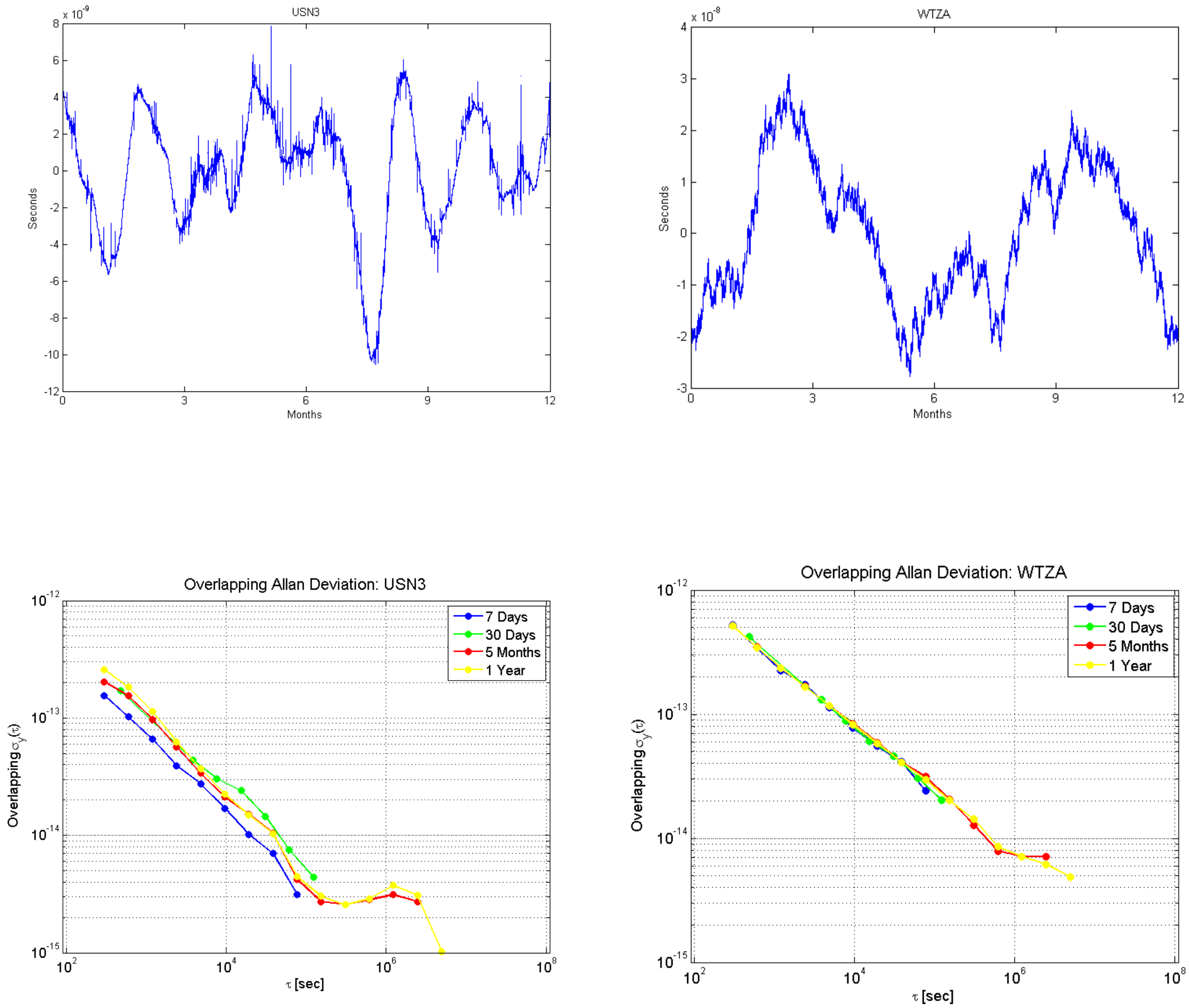

Figure 5.16: The two top figures show the estimated clocks for the stations USN3 and WTZA over one year period with GAPSTFT. The two bottom figures shows the frequency stability respectively for the two stations

After analyzing Figures 5.15 and 5.16 and Table 5.5, we can see the influence of the noise clock phase from stations NRC1 and ONSA in the frequency stability results of one year. Under normal circumstances, GAPSTFT indicated it can estimate a frequency stability at the level of 10^{-15} for short and long and term stability.

5.5 Assessment of time and frequency transfer performance (link)

In this section we will present an assessment of the GAPSTFT clock solutions using the "Clock comparison (link)" option provided by GAPSTFT. In other words, an assessment of time and frequency transfer performed (link) by GAPSTFT. By the word "link" we mean clock or frequency comparison (difference) between two different stations.

In this experiment, we will choose stations AMC2 and PTBB as the basis for the time links, which can be seen in Table 5.6.

The reason for that choice is to provide baselines of variable length, allowing us to make an analysis as to whether or not the length of the baselines can influence time and frequency transfer performance.

Table 5.6: Baselines for time and frequency transfer

		Length (Km)			Length (Km)
AMC2	**IENG**	8525	**PTBB**	**IENG**	813
	NIST	145		**NIST**	8000
	NRC1	2500		**NRC1**	6000
	ONSA	7825		**ONSA**	585
	PTBB	8141		**ROAP**	2195
	ROAP	8225		**USN3**	6560
	USN3	2400		**WAB2**	632
	WAB2	8385		**AMC2**	8525

5.5.1 Time Transfer Using GAPSTFT

In this subsection we will present an analysis of the time link solutions. The next two figures, 5.17 and 5.18 , show the time link between two stations. The links are divided between the two base stations AMC2 and PTBB. To perform the link, most outliers were removed and the gaps in the clock phase were filled using the GAPSTFT tools presented in Section 4.3.1.

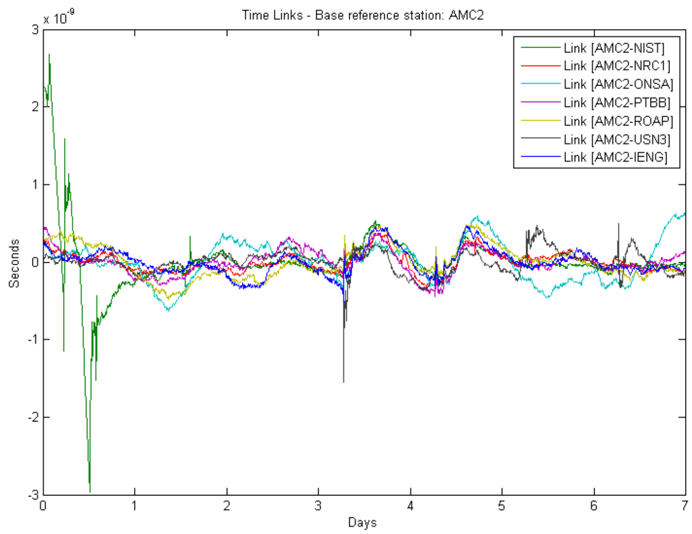

Figure 5.17: Link results for a period of 7-days with baselines related to station AMC2

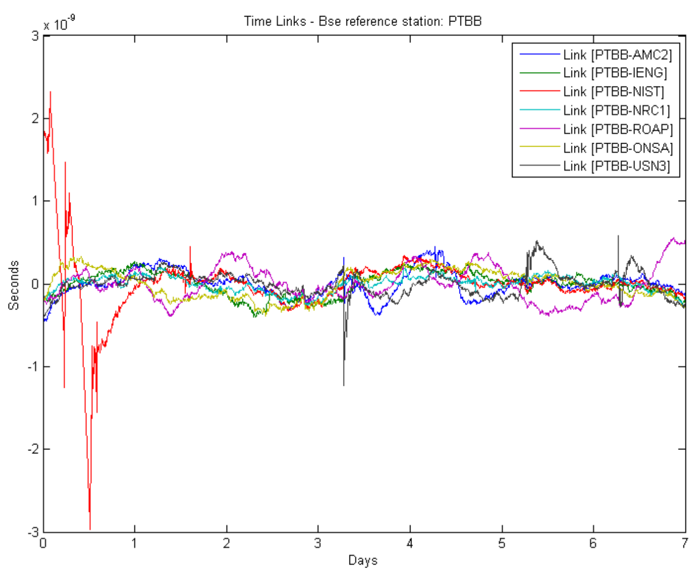

Figure 5.18: Link results for a period of 7-days with baselines stating from the station PTBB

On page 73, we told that stations with large gaps (e.g., USN3) were not to be used. In the next experiments we decided to include some of those stations in the results to show how the gaps could affect the clock-offset estimation using GAPSTFT.

Figures 5.17, 5.18 and 5.19 show all links. Large variation and slow convergence is found in NIST results. The convergence is due to the long periods of missing observation data in the first day of station NIST. The missing data results in ambiguity resets and then it reflects on the estimated clocks.

Links based on station USN3, also show some spikes due to missing observation data.

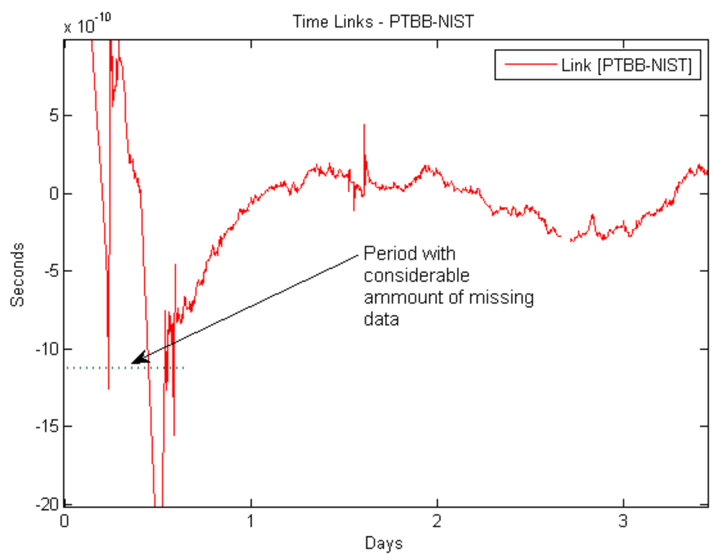

Figure 5.19: Results showing big variations for the time Link PTBB-NIST due to the missing data on the Station NIST

Still analyzing Figures 5.17 and 5.18, we can see a very accentuate sinusoidal results for the links based on the station AMC2 (Figure 5.17). Figure 5.18 also shows a sinusoidal results for the link involving station AMC2. Other sinusoidal results can be seen in the Figure 5.18 as well, but smother ones, such as ROAP and USN3.

The time community indicates that Geometrical Dilution of Precision(GDOP) and temperature as potential causes for variations in clock-offsets.

The GDOP can be defined as an indicator of three dimensional positioning accuracy as consequence of relative position of GPS satellites with respect to a GPS receiver or by the influence of the temperature on the estimated clocks.

No relation between the GDOP and the sinusoidal clock behaviors were found. However, after checking the temperature for the same 7 days of the experiment, a direct relationship between the temperature and the AMC2 estimated clock was found. Figure 5.20 display temperature and dew point variations.

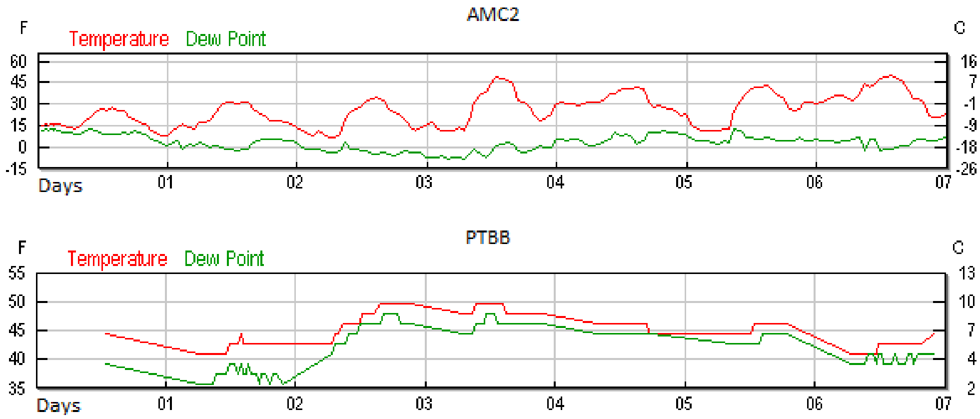

Figure 5.20: Temperature time series for the stations AMC2 and PTBB

The large amplitudes in the temperature of the station AMC2, seems to correlate to the sinusoidal behavior for the links which involves other stations that are being affected by the temperature as well. On the other hand, the links with station PTBB as base turned out to be smother due the little influence of the temperature on the station PTBB. Even though calibration is made. There are still residual variations left unaccounted in.

The next table provides a statistic analysis of the link results in comparison with the length of the baselines provided by the Table 5.7.

Table 5.7: Statistics values for time transfer for 7 days analysis

		Length (Km)	Std (s)	rms (s)
AMC2	**IENG**	8525	1.67 E-10	1.67 E-10
	NRC1	2500	1.29 E-10	1.29 E-10
	USN3	2400	2.64 E-10	2.64 E-10
	PTBB	8141	1.57 E-10	1.57 E-10
	ROAP	8225	2.14 E-10	2.14 E-10
	ONSA	7825	1.49 E-10	1.49 E-10
	NIST	145	4.46 E-10	4.46 E-10
PTBB	**IENG**	813	1.46 E-10	1.45 E-10
	NRC1	6000	9.72 E-11	9.71 E-11
	USN3	6560	2.09 E-10	2.09 E-10
	ROAP	2195	1.71 E-10	1.71 E-10
	ONSA	585	1.54 E-10	1.54 E-10
	AMC2	8525	1.57 E-10	1.57 E-10
	NIST	8000	4.09 E-10	4.09 E-10

The advantage of using PPP for time and frequency transfer is the lack of correlation between the link and the length of the baselines between the two selected stations, as we can see from the Table 5.7. We can get very similar STD values coming from very different baseline lengths, for instance: AMC2-NIST (145km) and PTBB-NIST (8000km).

5.5.2 Frequency transfer Using GAPSTFT

In this subsection we will present an analysis of the link frequency stability solutions provided by GAPSTFT. The analysis will be performed using the overlapping Allan deviation option available in GAPSTFT.

The solutions are based on the same links used in Table 5.6. The frequency offset and drift were removed from the clock-offset from each station before the links were performed. Also, most outliers present in the stations clock values were removed following the median absolute deviation (MAD), as explained in Chapter 4.

Figures 5.21 and 5.22 provide a frequency stability analysis using the overlapping Allan deviation for the links based on the stations AMC2 and PTBB. Table 5.8 provides the OADEV value for links at $\tau = 76800$ seconds.

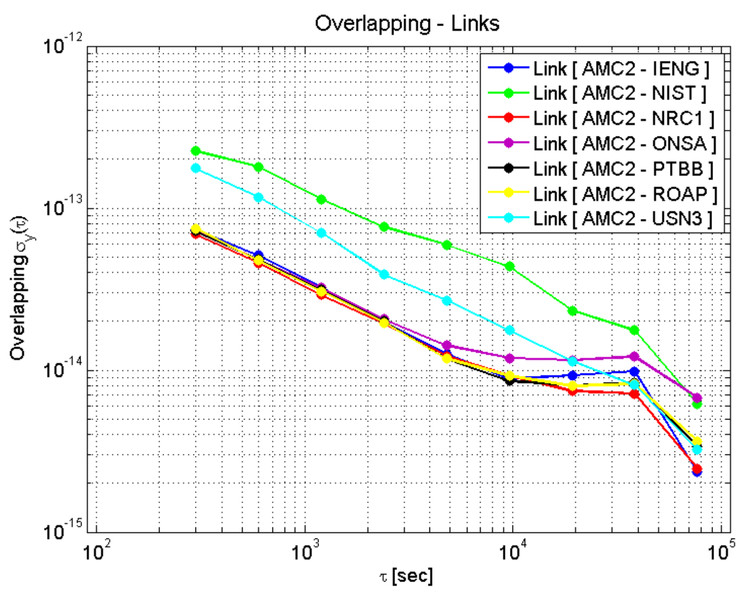

Figure 5.21: Overlapping Allan Deviation for frequency links for a period of 7-days - Link base AMC2

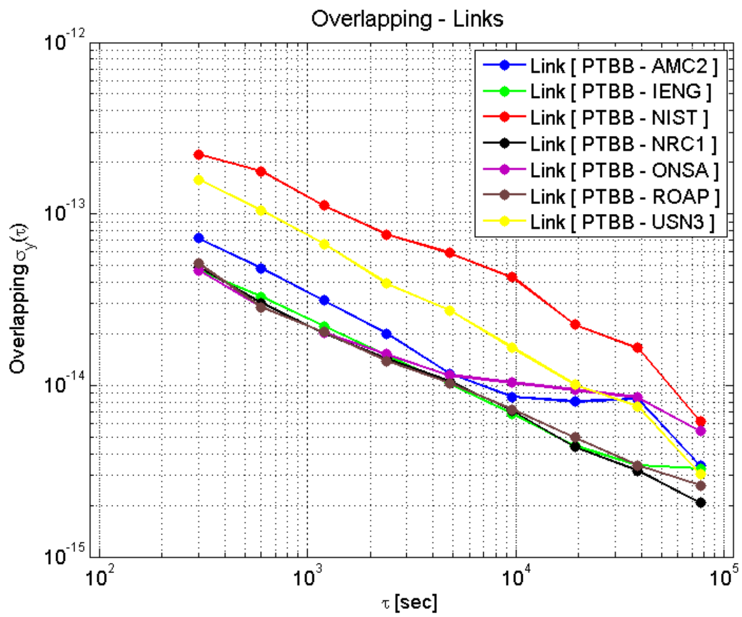

Figure 5.22: Overlapping Allan Deviation for frequency links for a period of 7-days - Link base PTBB

Table 5.8: Minimum overlapping ADEV value for links of 7 days: at τ = 76800 seconds

		Min OADEV			Min OADEV
AMC2	**IENG**	2.35 E-15	**PTBB**	**AMC2**	3.38 E-15
	NIST	6.14 E-15		**IENG**	3.27 E-15
	NRC1	2.47 E-15		**NIST**	6.13 E-15
	ONSA	6.75 E-15		**NRC1**	2.06 E-15
	PTBB	3.38 E-15		**ONSA**	5.41 E-15
	ROAP	3.64 E-15		**ROAP**	2.60 E-15
	USN3	3.22 E-15		**USN3**	3.02 E-15

Figures 5.21 and 5.22 and Table 5.8 show us that GAPSTFT is capable of providing a frequency stability at a magnitude of 10^{-15} for all the links. Links involving the stations NIST and USN3 present slightly less frequency stability before the convergence at $\tau = 76800$ seconds, which can be explained

by the considerable amount of missing observation for these two stations.

From the results presented in this subsection we conclude that GAPSTFT can provide a frequency stability at a magnitude of 10^{-15} for frequency transfer for short and long baselines. Also, GAPSTFT can provide all the output information related to the frequency stability analysis.

5.6 PPP Time Transfer versus P3 Common-View

In this section we will evaluate GAPSTFT comparing its results with the CV P3 method described in Chapter 3. The comparison will again being based on the links between the same stations for the same period as shown in Table 5.6.

The P3 results were obtained with the software called R2CGGTTS, version 5.1, available at the BIPM FTP. The results were calculated taking into account only GPS observations.

R2CGGTTS provides as results a estimated clock value for each in-view-satellite at each epoch at the rate of 16 minutes. As we want to test the CV P3 method between two stations (link), we subtract the estimated clock between the two common-view satellites at the same epoch, then we average all the results between the same epoch. By the end, we have a vector with the link results between the two stations for every 16 minutes.

It must be highlighted that our experiment with the P3 method for the link computations are being performed on various baseline lengths. The impact of long baselines on the common view method is a low number of common-view satellites between the two linked stations. Also, long baselines implies that the propagation paths are not identical between the two stations. The larger the baseline, the larger the differential propagation delays.

We can see in Figure 5.23 the clock-phases estimated with the P3 method plotted in the same figure.

Figure 5.23 shows a very large variation for the estimated clocks for the stations NIST when compared with the other stations. Due to this unexplained NIST clock behavior, we will not use the station NIST for the experiments in this subsection. Figure 5.24 shows comparisons between clock estimated values using the CV P3 method without station NIST.

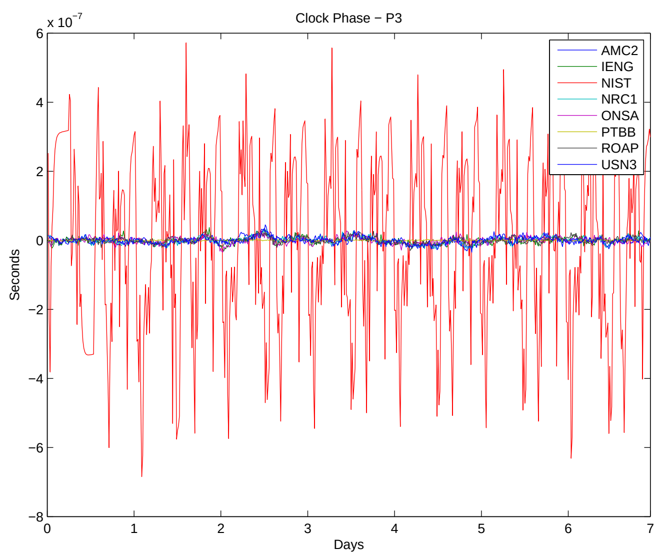

Figure 5.23: Estimated clock phases using CV P3 method

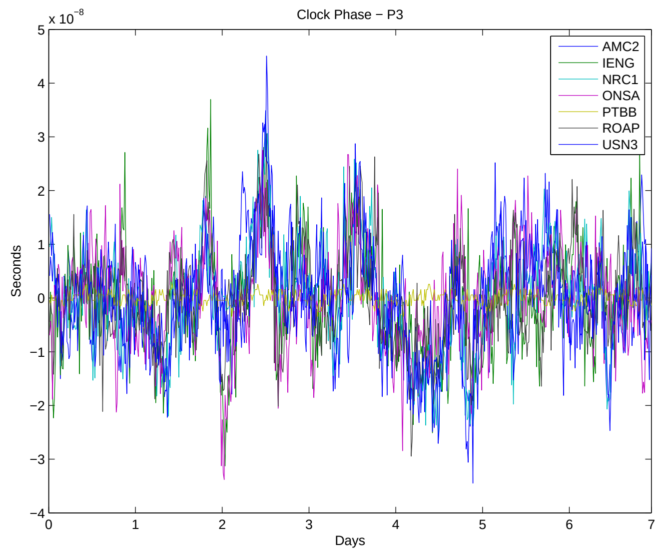

Figure 5.24: Estimated clock using CV P3 method

After using the software R2CGGTTS to estimate the clocks based on the CV-P3 method, we performed the time link between the stations. Table 5.9 shows the statistic values for the time link based on the CV P3 method following the baselines from Table 5.6. As we were expecting for the CV, the links show better results for the smaller baselines.

Table 5.9: Standard deviation and root mean square for the time links provided by the CV P3 method

		Distance (Km)	Std (s)	rms (s)
AMC2	**IENG**	8525	1.09 E-08	1.09 E-08
	NRC1	2500	7.48 E-09	7.47 E-09
	ONSA	7825	1.10 E-08	1.10 E-08
	PTBB	8141	9.69 E-08	9.68 E-08
	ROAP	8225	1.03 E-08	1.03 E-08
	USN3	2400	8.60 E-09	8.59 E-09
PTBB	**IENG**	813	9.09 E-09	9.08 E-09
	NRC1	6000	9.70 E-09	9.69 E-09
	ONSA	585	9.13 E-09	9.12 E-09
	ROAP	2195	9.23 E-09	9.22 E-09
	USN3	6560	1.00 E-08	1.00 E-08
	AMC2	8141	9.69 E-08	9.68 E-08

Table 5.10 compares statistic values for the time transfer results provided by R2CGGTTS (CV P3) and GAPSTFT (PPP). It shows better results for the PPP method for all baselines in comparison to the CV P3 method.

Table 5.10: Time Transfer comparison between CV P3 method and PPP using standard deviation and root mean square

		CV-P3 Std (s)	PPP Std (s)	CV-P3 rms (s)	PPP rms (s)
AMC2	**IENG**	1.09 E-08	1.67 E-10	1.09 E-08	1.67 E-10
	NRC1	7.48 E-09	1.29 E-10	7.47 E-09	1.29 E-10
	ONSA	1.10 E-08	2.65 E-10	1.10 E-08	2.65 E-10
	PTBB	9.69 E-08	1.57 E-10	9.68 E-08	1.57 E-10
	ROAP	1.03 E-08	2.15 E-10	1.03 E-08	2.15 E-10
	USN3	8.60 E-09	1.49 E-10	8.59 E-09	1.49 E-10
PTBB	**IENG**	9.09 E-09	1.46 E-10	9.08 E-09	1.46 E-10
	NRC1	9.70 E-09	9.72 E-11	9.69 E-09	9.72 E-11
	ONSA	9.13 E-09	2.09 E-10	9.12 E-09	2.09 E-10
	ROAP	9.23 E-09	1.71 E-10	9.22 E-09	1.71 E-10
	USN3	1.00 E-08	1.54 E-10	1.00 E-08	1.54 E-10
	AMC2	9.69 E-08	1.57 E-10	9.68 E-08	1.57 E-10

Another way of comparing GAPSTFT results with the CV P3 method is to analyze the frequency stability of the links using overlapping Allan deviation. Figures 5.25 and 5.26 show very consistent results for all the CV P3 links in terms of frequency stability analysis.

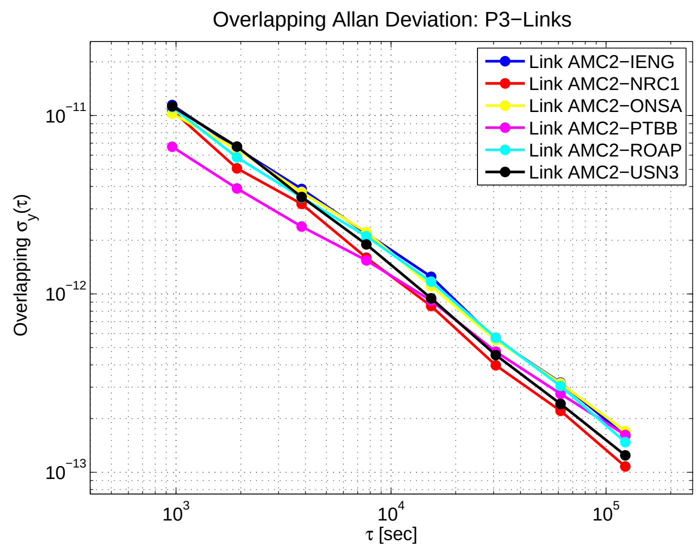

Figure 5.25: Frequency stability analysis using overlapping allan deviation for the CV-P3 Links - reference station AMC2

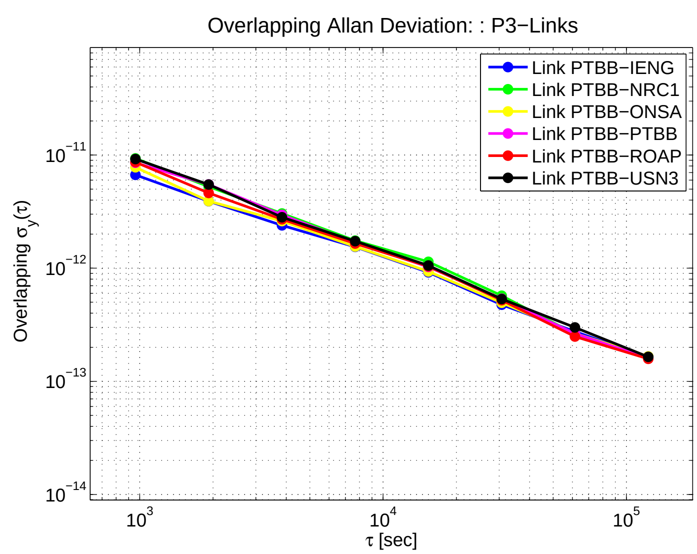

Figure 5.26: Frequency stability analysis using overlapping allan deviation for the CV-P3 - reference station PTBB

Table 5.11 presents a comparison between the minimum overlapping Allan Deviation values (OADEV) for the CV P3 and PPP methods. A visual comparison can also be made by looking at Figures 5.25 and 5.26.

Table 5.11: Minimum OADEV values for the frequency links at $\tau = 122880$ seconds for the CV-P3, and at $\tau = 76800$ seconds for the PPP

		CV-P3 (OADEV)	PPP (OADEV)
AMC2	**IENG**	1.60 E-13	2.35 E-15
	NRC1	1.08 E-13	2.47 E-15
	ONSA	1.71 E-13	6.75 E-15
	PTBB	1.62 E-13	3.38 E-15
	ROAP	1.48 E-13	3.65 E-15
	USN3	1.24 E-13	3.23 E-15
PTBB	**IENG**	1.63 E-13	3.27 E-15
	NRC1	1.66 E-13	2.07 E-15
	ONSA	1.61 E-13	5.41 E-15
	ROAP	1.58 E-13	2.60 E-15
	USN3	1.64 E-13	3.03 E-15
	AMC2	1.62 E-13	3.38 E-15

The frequency instability of the results presented in Table 5.11, expressed as the Overlapping Allan deviation (OADEV), shows a less stable frequency, in a order of two magnitudes for the CV P3 method when compared with PPP. Also, the PPP method achieves its best stability faster than the CV P3 method ($\tau = 76800$ seconds). Figures 5.27, 5.28, 5.29 and 5.30 show examples of some of data found in Table 5.11.

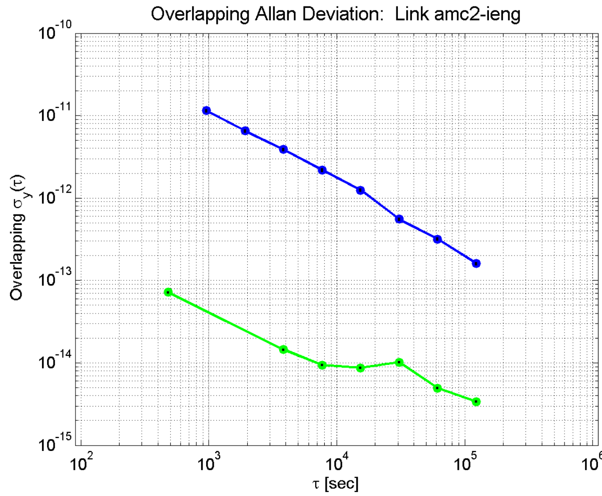

Figure 5.27: Comparison between CV P3 (blue) and PPP (green) expressed in OADEV: Link AMC2-IENG

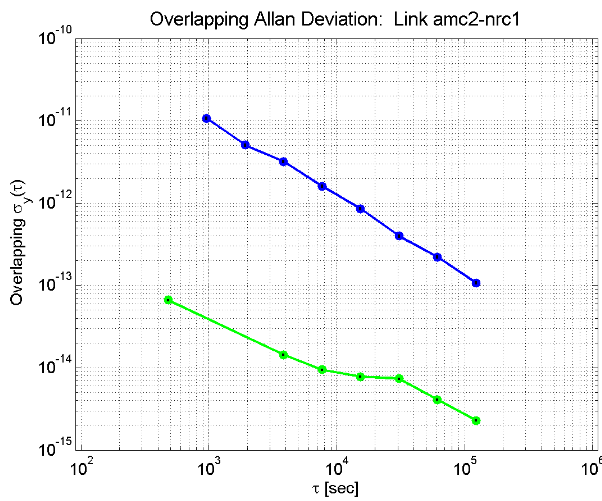

Figure 5.28: Comparison between CV P3 (blue) and PPP (green) expressed in OADEV: Link AMC2-NRC1

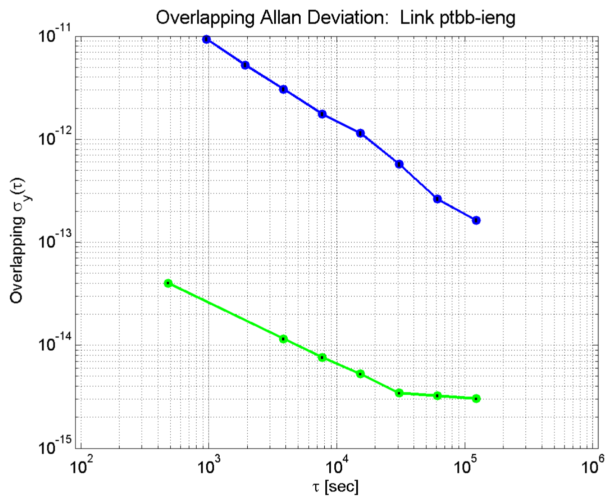

Figure 5.29: Comparison between CV P3 (blue) and PPP (green) expressed in OADEV: Link AMC2-IENG

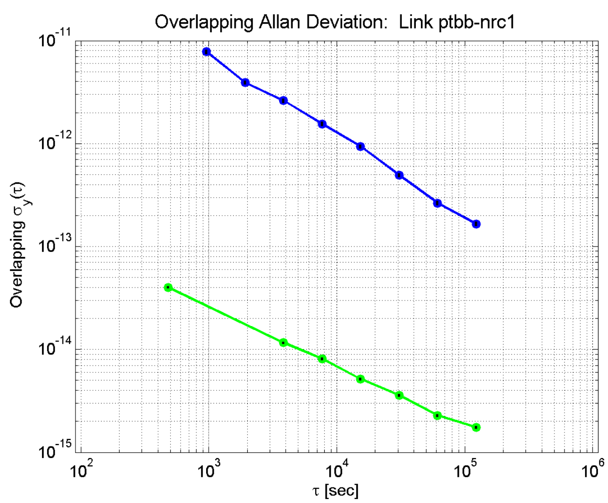

Figure 5.30: Comparison between CV P3 (blue) and PPP (green) expressed in OADEV: Link AMC2-NRC1

5.7 Comparison between GAPSTFT and NRCan PPP

In the last section of this chapter, the time and frequency results and links provided by GAPSTFT are compared with another PPP software that is made available the Natural Resources Canada (NRCan).

The NRCan-PPP software was chosen because it is the official PPP software used by the BIPM to provide the links contribution to the UTC and TAI. The NRCan-PPP has been updated frequently to provide the best estimated clock for time and frequency transfer. More details about the NRCan-PPP software and its updates for time and frequency transfer purpose can be found at Orgiazzi et al. [2005], Guyennon et al. [2009] and Cerretto et al. [2011].

Time Transfer (time Link) analysis

The NRCan-PPP version available for this experiment allows to process in multi-day continuous processing only up to six days. The estimated clocks in the first day is neglected due to the convergence time.

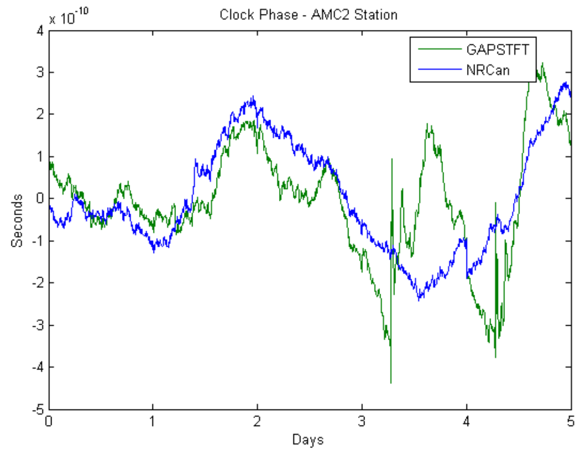

Figure 5.31: Estimated clocks by NRCan-PPP and GAPSTFT: Station AMC2

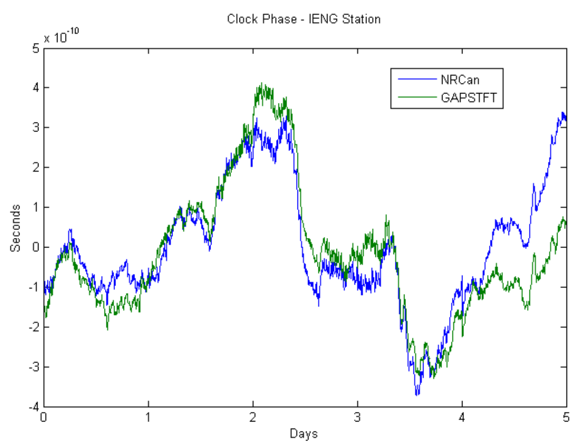

Figure 5.32: Estimated clocks by NRCan-PPP and GAPSTFT: Station IENG

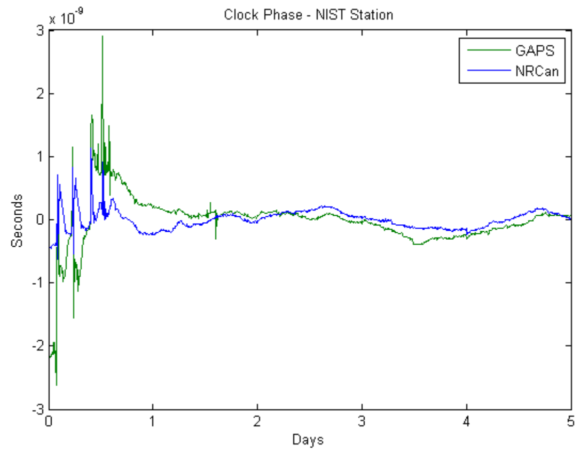

Figure 5.33: Estimated clocks by NRCan-PPP and GAPSTFT: Station NIST

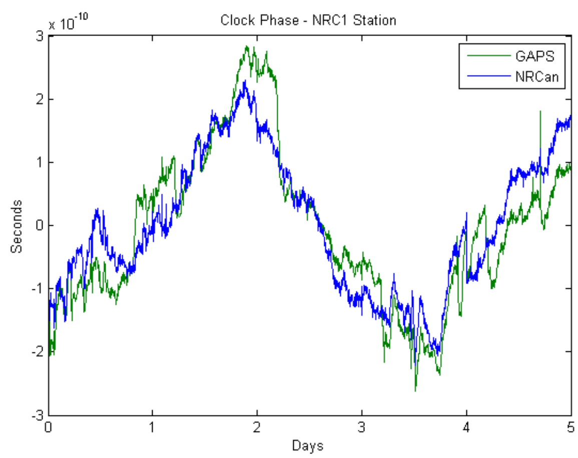

Figure 5.34: Estimated clocks by NRCan-PPP and GAPSTFT: Station NRC1

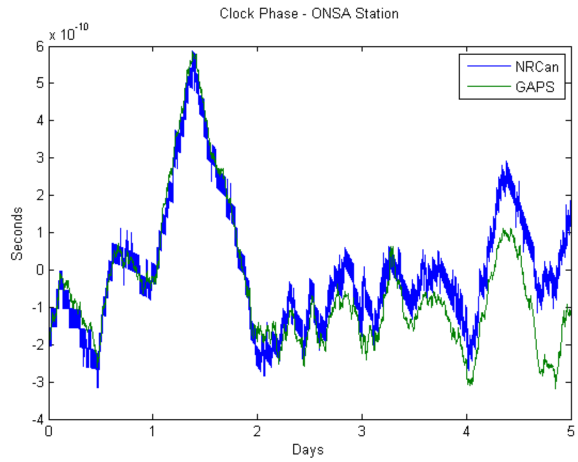

Figure 5.35: Estimated clocks by NRCan-PPP and GAPSTFT: Station ONSA

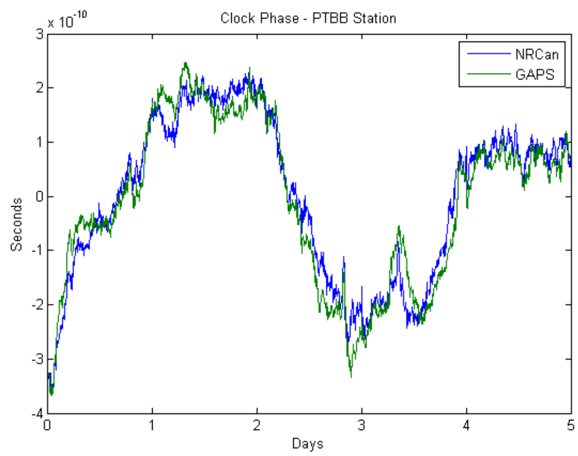

Figure 5.36: Estimated clocks by NRCan-PPP and GAPSTFT: Station PTBB

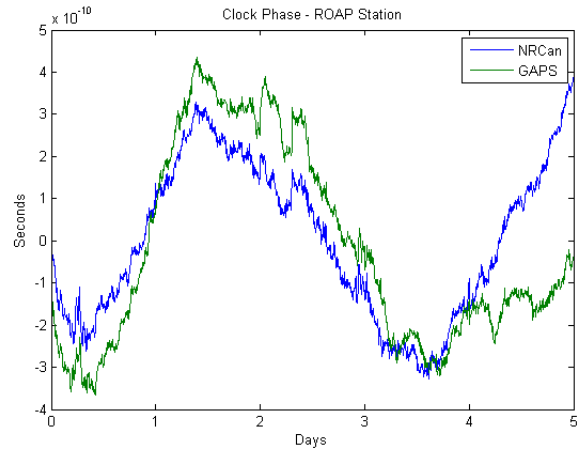

Figure 5.37: Estimated clocks by NRCan-PPP and GAPSTFT: Station ROAP

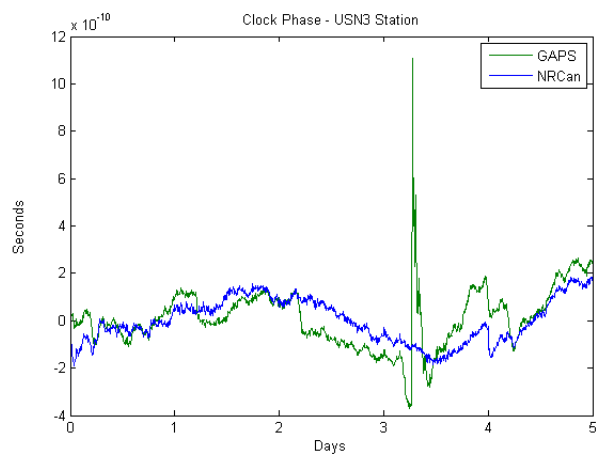

Figure 5.38: Estimated clocks by NRCan-PPP and GAPSTFT: Station USN3

The previous plots show the estimated clock provided by the two software suites. A visual analysis allow us to affirm that GAPSTFT and NRCan estimated clocks fallow each other in general. NRCan's solutions seems to be more stable overall.

Table 5.12: Standard deviation and rms values comparing the clock phases between GAPSTFT and NRCan-PPP

	GAPS-STD (s)	NRCan-STD (s)	GAPS-RMS (s)	NRCan-RMS (s)
AMC2	1.38 E-10	1.29 E-10	1.38 E-10	1.29 E-10
IENG	1.65 E-10	1.55 E-10	1.66 E-10	1.55 E-10
NIST	4.32 E-10	1.59 E-10	4.32 E-10	1.59 E-10
NRC1	1.22 E-10	1.07 E-10	1.22 E-10	1.07 E-10
ONSA	1.87 E-10	1.71 E-10	1.91 E-10	1.71 E-10
PTBB	1.50 E-10	1.48 E-10	1.50 E-10	1.48 E-10
ROAP	2.33 E-10	1.85 E-10	2.34 E-10	1.85 E-10
USN3	1.27 E-10	9.29 E-11	1.27 E-10	9.29 E-11

The statistic values from table 5.12 just confirm what the visual analysis of the plots indicated to us: the STD and RMS values for the NRCan-PPP are slightly smaller when compared with GAPSTFT.

As mentioned before, there are observation gaps in the first day of the estimated clocks for the station NIST. NRCan-PPP is capable of providing a smoother transition when observation gaps are presented in the clock phase (see Figure 5.33). A difference of 0.273 ns for station NIST was found when comparing the standard deviation values between the two GAPSTFT and NRCan-PPP.

Figures 5.39 and 5.40 show some spikes in the clock phase estimated by GAPSTFT at the same epochs, during day 3, for AMC2 and USN3 stations. Similar spikes are not present in the clock phase estimated by NRCan software. The carrier-phase residuals from the stations AMC2 and USN3 provided by GAPSTFT for each satellite were analyzed and some high carrier-phase values were found for satellites 3, 6 and 26, as we can see in Figures

5.39, 5.40, 5.41 and 5.42.

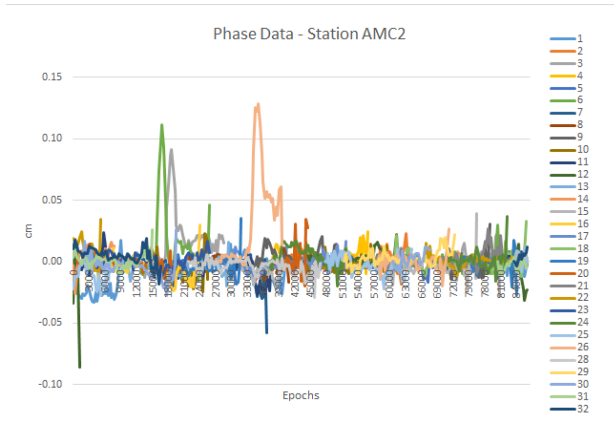

Figure 5.39: Carrier-phase residuals - Station AMC2 - all satellites

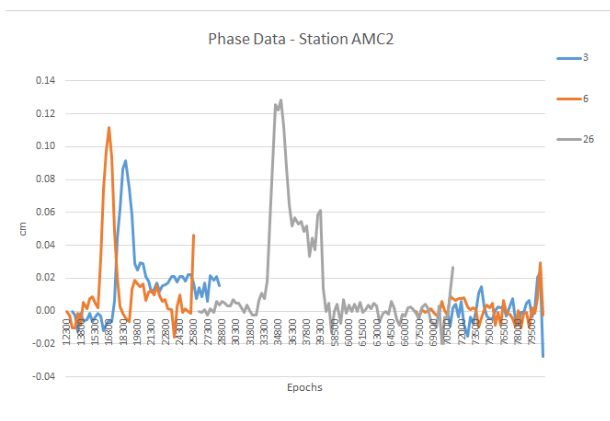

Figure 5.40: Carrier-phase residuals - Station AMC2 - satellites 3, 6, and 26

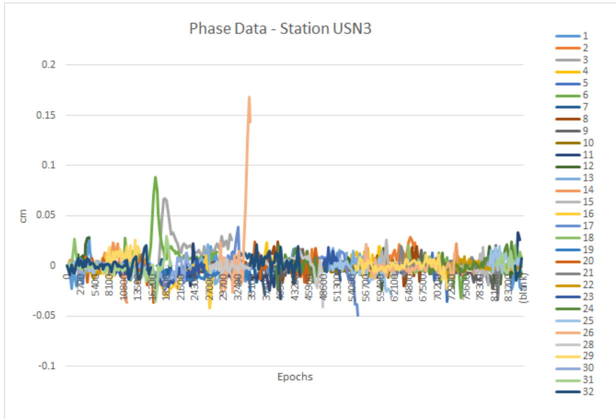

Figure 5.41: Carrier-phase residuals - Station USN3 - all satellites

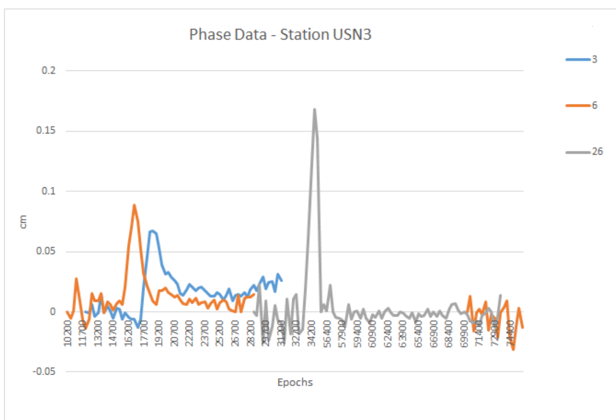

Figure 5.42: Carrier-phase residuals - Station USN3 - satellites 3, 6, and 26

Satellites 3, 6 and 26 were removed from the observation file from stations AMC2 and USN3 using program TEQC (Translation, Editing and Quality Checking) provided by UNAVCO. The files without the mentioned satellites were reprocessed by GAPSTFT. The new clock outputs kept the same spikes on both stations.

The ionospheric delay, multipath and troposphere values were also analyzed, but nothing was found out of the ordinary to explain those features. An explanation for the presence of the spikes only on the GAPSTFT clock solution may be the lack of the backward and smoothing solution, an approach that is present in the NRCan-PPP software.

Once we compared the estimated clocks from both software suites, we can also evaluate the time links between the same baselines that were used in the previous experiments in this chapter.

Table 5.13: Standard deviation and rms of GAPSTFT and NRCan-PPP time links.

		GAPSTFT STD (s)	RMS (S)	NRCan STD (s)	RMS (s)
AMC2	**IENG**	1.91E-10	1.91E-10	7.79E-11	7.78E-11
	NIST	4.49E-10	4.49E-10	1.51E-10	1.51E-10
	NRC1	1.45E-10	1.45E-10	6.98E-11	6.98E-11
	ONSA	2.43E-10	2.46E-10	2.13E-10	2.12E-10
	PTBB	1.82E-10	1.82E-10	1.42E-10	1.41E-10
	ROAP	2.44E-10	2.45E-10	1.20E-10	1.20E-10
	USN3	1.41E-10	1.41E-10	6.75E-11	6.75E-11
PTBB	**IENG**	1.67E-10	1.67E-10	1.38E-10	1.38E-10
	NIST	4.05E-10	4.05E-10	2.19E-10	2.19E-10
	NRC1	9.94E-11	9.94E-11	8.51E-11	8.51E-11
	ONSA	1.73E-10	1.76E-10	1.69E-10	1.69E-10
	ROAP	1.91E-10	1.92E-10	1.14E-10	1.14E-10
	USN3	1.33E-10	1.34E-10	1.01E-10	1.01E-10
	AMC2	1.82E-10	1.82E-10	1.42E-10	1.41E-10

Frequency Transfer (frequency link) Analysis

The next analysis was based on a comparison between the frequency link results provided by GAPSTFT and NRCan-PPP for the same period of five days.

Table 5.14: Minimum overlapping ADEV values at tau = 76800 seconds

		GAPSTFT	NRCan
AMC2	**IENG**	2.29E-15	1.29E-15
	NIST	7.63E-15	2.64E-15
	NRC1	2.27E-15	1.87E-15
	ONSA	6.29E-15	6.61E-15
	PTBB	3.32E-15	3.47E-15
	ROAP	3.99E-15	3.10E-15
	USN3	2.86E-15	1.99E-15
PTBB	**IENG**	3.83E-15	3.64E-15
	NIST	7.66E-15	5.35E-15
	NRC1	2.35E-15	2.09E-15
	ONSA	4.96E-15	5.35E-15
	ROAP	3.09E-15	2.87E-15
	USN3	2.54E-15	2.61E-15
	AMC2	3.32E-15	3.47E-15

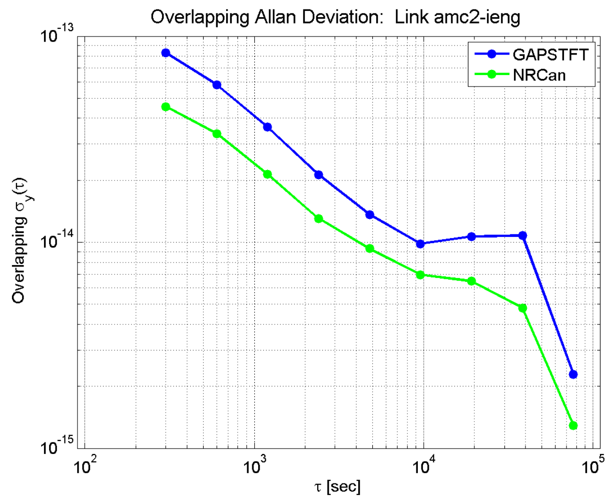

Figure 5.43: OADEV for the links AMC2-IENG

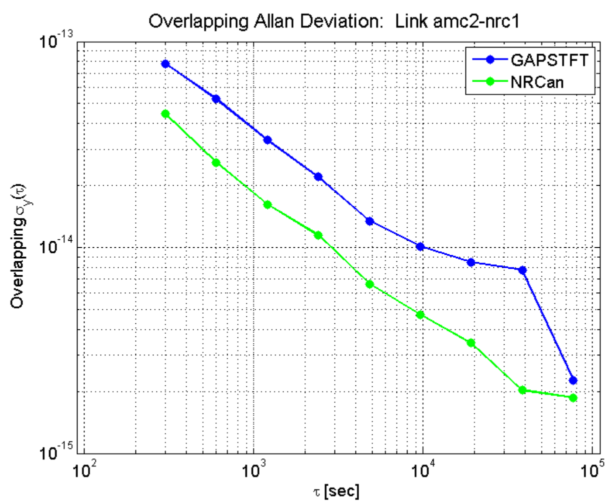

Figure 5.44: OADEV for the links AMC2-NRC1

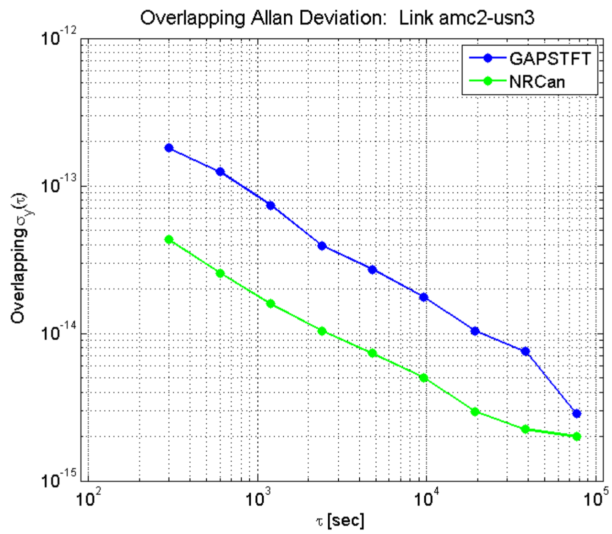

Figure 5.45: OADEV for the links AMC2-ONSA

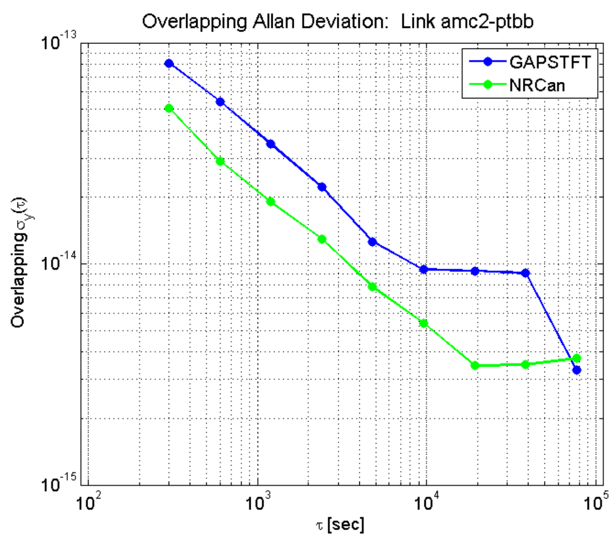

Figure 5.46: OADEV for the links AMC2-PTBB

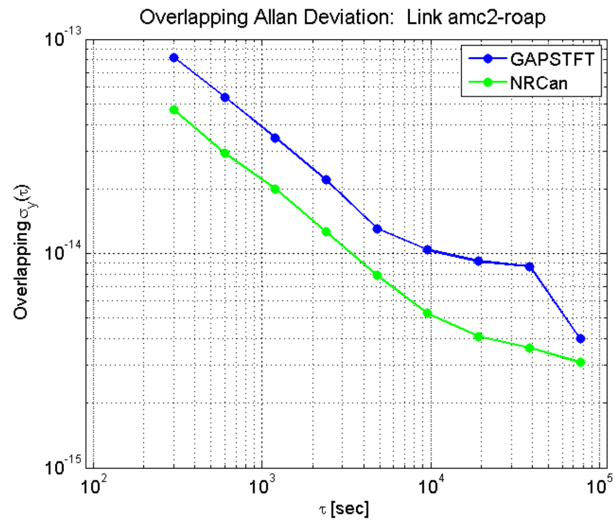

Figure 5.47: OADEV for the links AMC2-ROAP

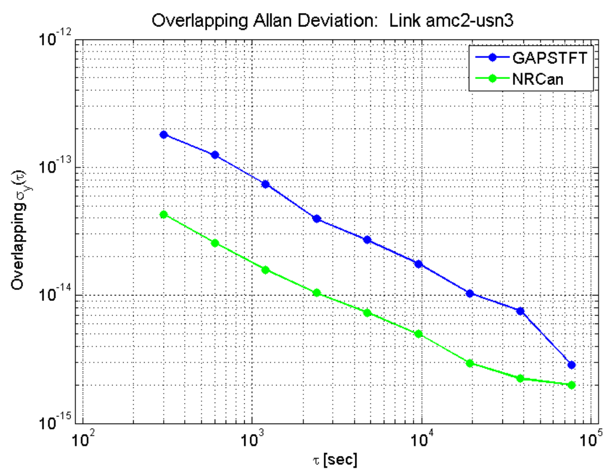

Figure 5.48: OADEV for the links AMC2-USN3

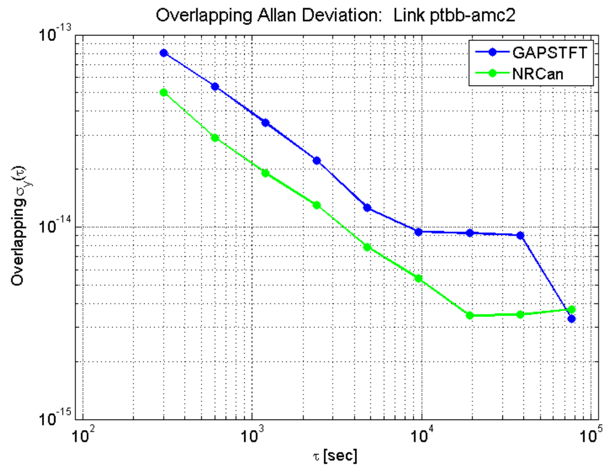

Figure 5.49: OADEV for the links PTBB-AMC2

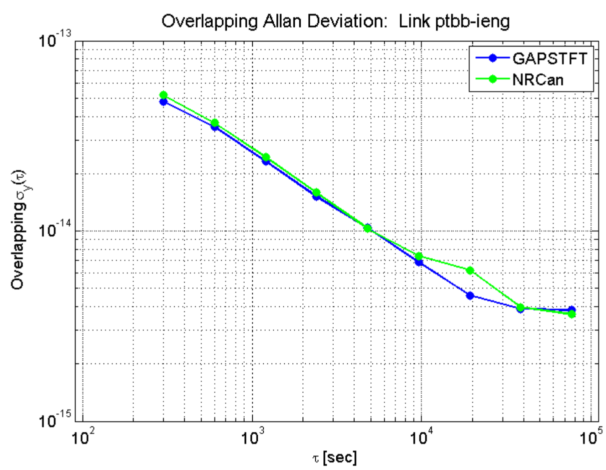

Figure 5.50: OADEV for the links PTBB-IENG

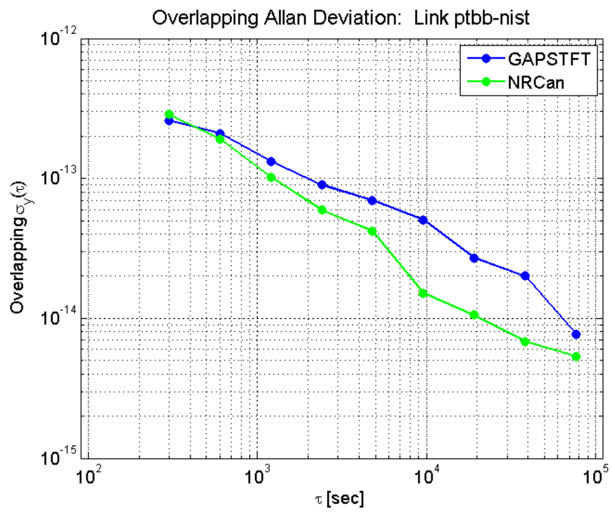

Figure 5.51: OADEV for the links PTBB-NIST

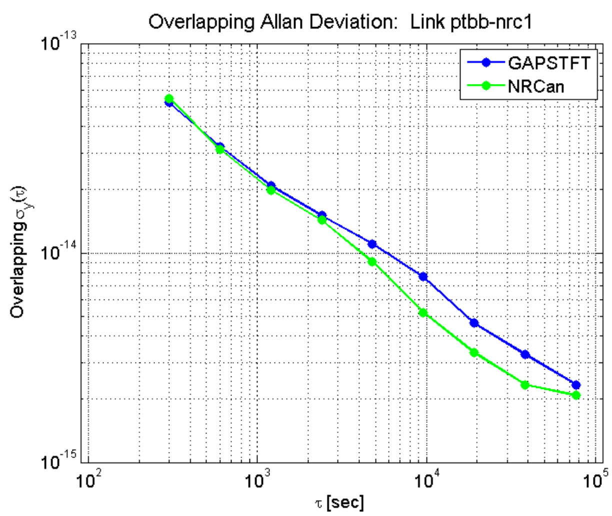

Figure 5.52: OADEV for the links PTBB-NRC1

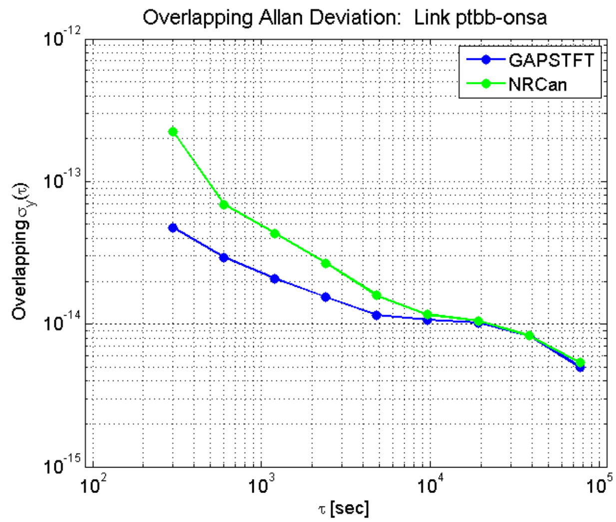

Figure 5.53: OADEV for the links PTBB-ONSA

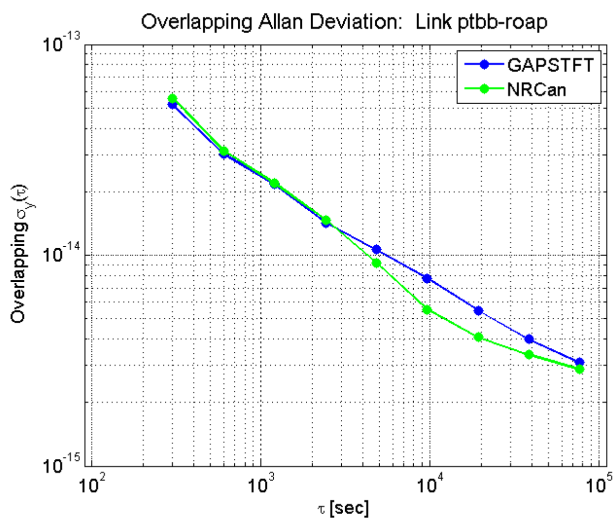

Figure 5.54: OADEV for the links PTBB-ROAP

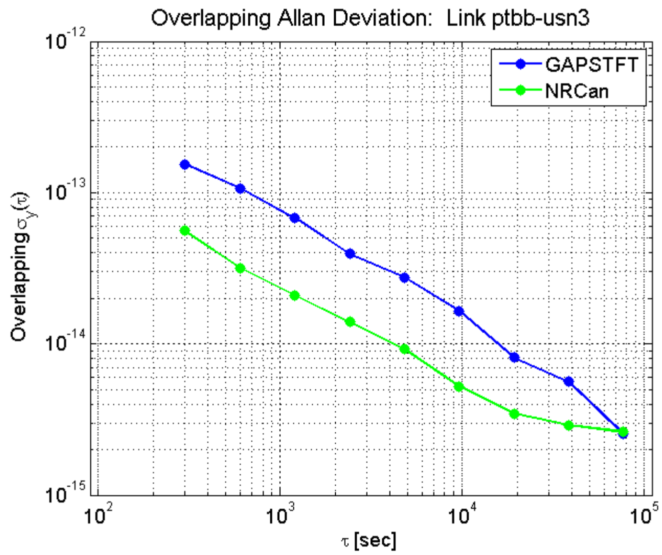

Figure 5.55: OADEV for the links PTBB-USN3

Figures 5.43 to 5.55 and Table 5.14 show that both GAPSTFT and NRCan can provide a frequency stability of 10^{-15} for periods of 5 days. However, NRCan-PPP seems to provide slightly better frequency stability results than GAPSTFT.

5.8 Summary

This chapter was intended to provide a full assessment of GAPSTFT and its capability of being used as a tool for time and frequency transfer.

GAPSTFT assessment showed good performance based on what is expected by a conventional PPP for time and frequency. It proved to have a better performance then the P3 method for longer baselines nowadays. GAP-

STFT is capable of achieving 10^{-15} link frequency stability in both short and long term (for up to one year). When compared with other PPP software (NRCan-PPP), GAPSTFT link results showed a good agreement between the two softwares, but it also showed NRCan's be more stable overall.

Chapter 6

Closing Remarks

The main objective for this thesis was achieved. GAPSTFT is now a software with tested capabilities of performing time and frequency transfer using PPP post-processing and GPS signals.

First, an experiment was performed in order to test the development of the multi-day continuous processing. Seven consecutive random days were chosen and processed. By the achieved results, we could see that the Px matrix propagation, from the last epoch of a day to the first epoch of the next day, resulted in a smooth transition and allowed us to estimate clock values for several consecutive days without the day boundary discontinuity problem. The standard deviation of the solution decreased from a factor of 2 to 10 times with the newly developed method.

The next experiment was to test GAPSTFT capability of estimating clocks using the IGRT products. Before this implementation, GAPSTFT users had to wait for approximately 12 days for the IGST products to be available to estimate the clocks. Now, GAPSTFT users can use the IGRT products, which offers technically the same precision than the IGST products, but the wait time was brought down to 17 hours.

Regarding the third experiment, we implemented on GAPSTFT the option to estimate clocks at the lowest rate of 30 seconds, instead of the 5 minutes only. This option plays an important role for the frequency transfer users. It allows the users to perform a frequency stability analysis with a better confiability for short periods, such as one day.

On the fourth experiment, GAPSTFT software was tested in terms of estimating clocks and providing frequency stability for short and long periods of time. For the experiments involving the precision of the estimated clocks for different periods, GAPSTFT provided a std values at the magnitude of 10^{-10} for short periods, such as 7 days, and a std values at the magnitude of 10^{-09} for long periods, such as 1 year. On the frequency stability tests, GAPSTFT provided OADEV values at the magnitude of 10^{-15} for both short and long periods of time.

The fifth experiment were based on the assessment and evaluation of GAPSTFT to perform time and frequency transfer. The experiments were focused on using links with different baseline lengths. The results showed that GAPSTFT can reach the magnitude of 10^{-10} in terms of std values for time links, for both short and long baselines. In terms of frequency stability, GAPSTFT provided OADEV values at 10^{-15} for also both short and long baselines.

The last two experiments were performed on comparing GAPSTFT results with other GNSS time and frequency method (CV P3), and also, with other PPP software.

GAPSTFT provided better time and frequency values when compared with the CV P3 method for all links. In terms of clock values, GAPSTFT presented std values at the magnitude of 10^{-10} against 10^{-09} for the CV P3. In terms of frequency stability, GAPSTFT showed OADEV values at the magnitude of 10^{-15} against 10^{-12} for the CV P3 method. GAPSTFT also showed that its results are not limited by the baselines lengths. On the other hand, the CV P3 method presents better results for short baselines.

The last experiment compared GAPSTFT with the PPP software provided by the NRCan. The results from both software presented results at the same magnitude for both time and frequency transfer analysis. However, NRCan-PPP showed to be capable of presenting sometimes better results than GAPSTFT, for instance, NRCan-PPP showed to handle better when a station present some amount of missing observation data.

The clock estimation inside GAPSTFT is treated as white noise with a very small number used as uncertainty. It is possible that the clock absorbs some noise and/or some systematic signals during the estimation process. It could maybe explains the noise and the spikes in the GAPSTFT estimated clock. A method presented by Cerretto et al. [2010] would be recommended to investigate this issue. This method takes into account known behavior and noise characteristics of the atomic clocks frequency. The method is based on an implementation of constrained clock models. The results proved that the method can reduce by 1 to 2 orders of magnitude the noise for short-term for stations driven by Hydrogen-Masers only.

By the end, this work contributes providing a practical PPP package (GAPSTFT) at hand, focused on offering time and frequency transfer results, instead of positioning results as the original GAPS package. The implementations made on GAPSTFT, bring this package to offer time and frequency transfer stability at the same level, than the other PPP packages available. The evaluation of results shows that GAPSTFT can offer good time and frequency stability results for long short (one day) and long term (up to one year). GAPSTFT can offer to the user, a unique experience of having a desktop PPP package, capable of processing GPS data for two stations, perform time and frequency transfer results, and provide also all the tools for a time and frequency analysis. Thanks to these contributions, GAPSFTF is not only a package to provide time and frequency transfer results, but also, a software to test any kind of PPP development in the feature, and its impact on the estimated clock offsets.

Finally, by reviewing GAPSTFT development and assessment experiments, we can conclude that this work was successful. Further improvements are expected and can be reached by implementing multi-constellation capabilities as shown by [Defraigne et al., 2011] and [Defraigne et al., 2013], or by implementing an ambiguity fixing method based on what is called "Zero difference GPS ambiguity resolution". This method has been implemented on the NRCan-PPP software at the BIPM. The same method has also been implemented by [Martinez-Belda et al., 2012] on the PPP software called Atomium.

Bibliography

Allan, D. W., Ashby, N., and Hodge, C. C. (1997). The Science of Timekeeping: HP Application Note 1289. Miami, Florida, U.S.A.

Allan, D., and Weiss, M. (1980). “Accurate time and frequency transfer during common-view of a GPS satellite.” Paper presented at the 34th Annual Frequency Control Symposium. Philadelphia, Pennsylvania, U.S.A.

Bishop, R. H. (2002). *The Mechatronics*. Austin, Texas. U.S.A.

Blair, B. E. (1974). *Time and Frequency: Theory and Fundamentals*. Boulder, CO. U.S.A.

Cerretto, G., Lahaye, F., and Guyennon, N. (2008). “Precise Point Positioning for timing”. *Proceedings URSI - XXIX General Assembly*. Chicago, Il, U.S.A. pp. 3-6.

Cerretto, G., Lahaye, F., Tavella, P., and Vitrano, S. (2010). “Precise Point Positioning: Implementation of the constrained clock model and analysis of its effects in T/F transfer”. 24th European Frequency and Time Forum. pp. 1–5. Noordwijk, Netherlands.

Costa, R., Orgiazzi, D., Pettiti, V., Sesia, I., and Tavella, P. (2004). “GPS Common view data processing algorithm”. Istituto Nazionale di Ricerca Metrologica. Technical Report 667. Italy.

Dach, R., Hugentobler, U., Schildknecht, T., Bernier, L. G., and Dudle, G. (2005). "Precise continuous time and frequency transfer using GPS carrier phase." Proceedings of the 2005 IEEE International Frequency Control Symposium and Exposition, 2005. Vancouver, Canada.

David W. Allan, Dick D. Davis, M. Weiss, A. Clements, Bernard Guinot, Michel Granveaud, K. Dorenwendt, B. Fischer, P. Hetzel, Shinko Aoki, Masa-Katsu Fujimoto, and L. Charron, N. A. (1985). "Accuracy of International Time and Frequency Comparisons Via Global Positioning System Satellites in Common-View". *IEEE Transactions on Instrumentation and Measurement*.

Defraigne, P., Aerts, W., Harmegnies, A., Petit, G., Rovera, D., and Uhrich, P. (2013). "Advances in multi-GNSS time transfer". 2013 Joint European Frequency and Time Forum & International Frequency Control Symposium (EFTF/IFC). pp. 508–512. Prague, Czech Republic.

Defraigne, P., and Baire, Q. (2011). "Combining GPS and GLONASS for time and frequency transfer". *Advances in Space Research.* Vol. 47, No. 2, pp. 265-275.

Defraigne, P., Petit, G., and Bruyninx, C. (2002). "Use of geodetic receivers for TAI". 33rd Annual Precise Time and Time Interval (PTTI) Meeting. Long Beach, CA, U.S.A.

Delporte, J., Mercier, F., and Cnes, F. P. (2012). "Time Transfer with Integer PPP (IPPP)". *In Sevemth Meeting of the International Committee on Global Navigation Satellite Systems (ICG)*. Beijing, China.

El-Rabbany, A. (2002). *Introduction to GPS - The Global Positioning System*. Artech House. Norwood.

Feldmann, T. (2011). *Advances in GPS based Time and Frequency Comparisons for Metrological Use*. Ph.D. dissertation, Physikalisch-Technische Bundesanstalt. Leibniz University of Hannover, Germany.

Gurtner, W. and L. Estey (2006). “RINEX: The Receiver Independent Exchange Format Version 2.11”. Document available online at ftp://igscb.jpl.nasa.gov/pub/data/format/rinex211.txt, accessed on June 02, 2014.

Guyennon, N., Cerretto, G., Tavella, P., and Lahaye, F. (2009). “Further characterization of the time transfer capabilities of precise point positioning (PPP): the Sliding Batch Procedure”. *IEEE Transactions on Ultrasonics, Ferroelectrics, and Frequency Control*. Vol 56, No 8, pp. 1634 - 1641.

Héroux, P., and Kouba, J. (2001). “GPS precise point positioning using IGS orbit products”. *Physics and Chemistry of the Earth, Part A: Solid Earth and Geodesy.* Vol 26, No 6–8, pp 573–578.

Hewlett Packard. (1997). *The Science of Timekeeping*. Englewood, CO.

J. Wu, S. Wu, G. Hajj, and W. Bertiguer, S. L. (1993). “Effects of antenna orientation on GPS carrier phase”. Paper presented at the AAS/AIAA Astrodynamics Conference. Durango, Colorado, U.S.A.

Jespersen, J., and Fitz-Randolph, J. (1999). *From sundials to atomic clocks: understanding time and frequency*. Dover Publications. Mineola, U.S.A.

Jiang, Z., and Petit, G. (2004). “Time transfer with GPS satellites all in view”. Paper presented at the ATF2004. Beijing, China.

Kouba, J. (2009). “A guide to using International GNSS Service (IGS) products”. *Geodetic Survey Division Natural Resources Canada*. Ottawa. Vol. 6. pp. 34.

Kouba, J. A. N., and Heroux, P. (2001). “Precise Point Positioning Using IGS Orbit and Clock Products.” *GPS Solutions*, Vol. 5, No. 2, pp. 12-28.

Leandro, R. F. (2009). *Precise Point Positioning with GPS: A New Approach for Positioning, Atmospheric Studies, and Signal Analysis*. Ph.D. dissertation, Department of Geodesy and Geomatics Engineering, University of New Brunswick, Fredericton, N.B., Canada, 232 pp.

Leandro, R. F., Santos, M. C., and Langley, R. B. (2010). "Analyzing GNSS data in precise point positioning software". *GPS Solutions*, Vol. 15, No. 1, pp. 1-13.

Leandro, R., Santos, M., and Langley, R. (2007). "GAPS: The GPS analysis and positioning software - A brief overview". *Proceedings of the 20th International Technical Meeting of the Satellite Division of The Institute of Navigation (ION GNSS 2007).* Fort Worth, Texas, U.S.A., pp. 25–28.

Levine, J. (2008). "A review of time and frequency transfer methods". *Metrologia*, Vol. 45, No. 6, pp. S162-S174.

Lombardi, M. A. (2002a). "Chapter 17. Fundamentals of Time and Frequency". In *The Mechatronics Handbook.* Austin, Texas, U.S.A.

Lombardi, M. A. (2002b). Chapter 18. Time Measurement. In *The Mechatronics Handbook*. Austin, Texas, U.S.A.

Lombardi, M. A. (2002c). Chapter 19. Frequency Measurement. In *The Mechatronics Handbook*. Austin, Texas, U.S.A.

Lombardi, M. A. (2008). "The Use of GPS Disciplined Oscillators as Primary Frequency Standards for Calibration and Metrology Laboratories". *Measure*, Vol. 3, No. 3, pp. 56 – 65.

Lombardi, M., and Nelson, L. (2001)."Time and frequency measurements using the global positioning system". Paper presented at the Measurement Science Conference. pp. 26–33.

Martínez-Belda M. C.; Defraigne P. (2012). Precise Point Positioning with integer ambiguities in the Atomium software. In *PPP Workshop: Reaching Full Potential* (p. 2). Ottawa, ON. Canada.

Matsakis, D., Lee, M., Dach, Hugentobler, U., and Jiang, Z. (2006). "GPS Carrier Phase Analysis Noise on the USNO-PTB Baselines". Paper presented at the 2006 IEEE International Frequency Control Symposium and Exposition, pp. 631–636.

Orgiazzi, D., Tavella, P., and Lahaye, F. (2005). "Experimental assessment of the time transfer capability of Precise Point Positioning (PPP)". *Proceedings of the IEEE International Frequency Control Symposium and Exposition (2005).* Vol. 2005. pp. 337-345

Petit, G., and Arias, E. F. (2009). "Use of IGS products in TAI applications". *Journal of Geodesy*, Vol. 83, No. 3-4, pp. 327-334.

Petit, G., & Luzum, B. (2010). "The IERS Conventions (2010): Reference Systems and New Models". IERS Technical Note 36. Available at http://62.161.69.131/iers/convupdt/convupdt.html . Accessed on 21 September 2014.

Plumb, J., and Larson, K. (2005). "Absolute calibration of a geodetic time transfer system". *IEEE Transactions on Ultrasonics, Ferroelectrics, and Frequency Control.* Vol. 52, No. 11, pp. 1904-1911.

Riley, W. J. (2003). "Techniques for Frequency Stabilities Analysis". Paper presented at the IEEE International Frequency Control Symposium. Tampa, FL., U.S.A.

Riley, W. J. (2008). *Handbook of Frequency Stability Analysis* (p. 112). Boulder, CO.: NIST Special Publication 1065.

Scherneck, H. F. H. W. (1998). "Ocean Tide Loading and Diurnal Tidal Motion of the Solid." IERS Technical Note (25).

Grunert, Ulrich and Thölert, Steffen and Denks, Holmer and Furthner, Johann (2008). "Absolute Calibration of Time Receivers with GPS/Galileo HW Simulator". Paper presented at the 2008 Toulouse Space Show, Toulouse, France.

Vanícek, P. and E. J. K. (1986). *Geodesy: The Concepts*. North-Holland, Amsterdam.

Vita

Candidate's full name: Carlos Alexandre Garcia

University attended: University of New Brunswick
Fredericton, NB, Canada
September 2009 - January 2015
M.Sc.E. Geodesy and Geomatics Engineering

University of State of Sao Paulo - UNESP
Presidente Prudente, SP, Brazil
February 2002 - December 2006
Bachelor of Science in Geomatics Engineering